

ABSTRACT

HODY, JAMES WAGNER. Canid Collision – Range Expansion by Coyotes (*Canis latrans*) and Crab-eating Foxes (*Cerdocyon thous*) in Panama and Interpretation of Camera Trap Data. (Under the direction of Dr. Roland Kays).

Global environmental change poses a serious challenge for the conservation of biodiversity, and has created a need for rapid, effective surveys of ecological communities. Such surveys have traditionally been difficult for terrestrial mammals, but passive sampling devices such as camera traps have proven to be exceptionally useful for collecting large volumes of data on multiple species simultaneously. Despite the utility of the technique, many camera trapping studies are designed and analyzed without sufficient consideration for the underlying process generating the animal detection data, which could potentially lead to weakened ecological inferences. We empirically described the photographic detection process for four mammal species (white-tailed deer, *Odocoileus virginianus*; northern raccoon, *Procyon lotor*; coyote, *Canis latrans*; and gray fox, *Urocyon cinereoargenteus*) using animal movement data from a fine-scale camera trapping grid in Schenck Memorial Forest, North Carolina. We compared these observations against critical assumptions of occupancy models, one of the most common analytical tools used for analyzing camera trap data. We found that animal movement was nonrandom at the fine spatial scale sampled by camera traps characterized by species-specific movement corridors and hotspots of activity, and that camera traps frequently failed to photograph passing animals. We conclude that species detection probabilities may vary over short spatial distances, and that single cameras may poorly represent their surrounding areas. Arrays of camera traps may be more useful when studying broad-scale ecological processes. We implemented these recommendations in a camera trap survey in a rapidly changing Central American landscape. In recent decades,

coyotes and crab-eating foxes (*Cerdocyon thous*) have expanded their geographic ranges into newly deforested areas in Panama. Neither coyotes nor crab-eating foxes have historically occurred in Panama, and potential competition between the species and effects on local wildlife have not previously been investigated. We deployed camera trap arrays across eastern Panama and conducted opportunistic roadkill surveys to document the current spatial distribution of the two species, their daily activity patterns, and broad-scale habitat associations. We found that both species now overlap in agricultural areas between the Panama Canal and Lago Bayano, marking the first ever interaction between the two canids. Both species are predominantly nocturnal in eastern Panama, with a high degree of temporal overlap in their activity patterns. The two species were observed in similar habitats but were not observed to co-occur at any site, perhaps suggestive of spatial avoidance. Interestingly, coyote morphology documented in photographs suggests possible hybridization with feral dogs (*Canis familiaris*). Additional research will be needed to determine how coyotes and crab-eating foxes will interact once local populations become more established, but preliminary evidence suggests possible competition.

© Copyright 2016 by James Wagner Hody

All Rights Reserved

Canid Collision – Range Expansion by Coyotes (*Canis latrans*) and Crab-eating Foxes
(*Cerdocyon thous*) in Panama and Interpretation of Camera Trap Data

by
James Wagner Hody

A thesis submitted to the Graduate Faculty of
North Carolina State University
in partial fulfillment of the
requirements for the degree of
Master of Science

Fisheries, Wildlife, and Conservation Biology

Raleigh, North Carolina

2016

APPROVED BY:

Dr. Roland Kays
Committee Chair

Dr. Luther Scott Mills

Dr. Jamian Krishna Pacifici

DEDICATION

To my family, for their love, support, and encouragement every step along the way.

BIOGRAPHY

James Hody grew up in Bel Air, Maryland. His experiences with hiking, bird watching, and wildlife photography while growing up in this area fostered a lasting interest in ecology and conservation, which he pursued as an undergraduate at Virginia Tech. His studies and undergraduate research experiences here fed a growing interest population ecology, tropical ecology, and carnivore conservation. He graduated *summa cum laude* with a Bachelor's of Science in Wildlife Science and a minor in Mathematics in 2013, subsequently working as a research technician in Virginia and Wyoming. In fall 2014, he joined the Fisheries, Wildlife, and Conservation Biology Program at North Carolina State University under the direction of Dr. Roland Kays, where he studied methods for analyzing camera trap data and canids' responses to rapid land use changes in Central America.

ACKNOWLEDGMENTS

This thesis was supported by many people, both at NC State University and elsewhere. I would like to thank my advisor, Dr. Roland Kays, for giving me this opportunity and guiding me during my research at NC State University, and Dr. Scott Mills and Dr. Krishna Pacifici for their input and advice, particularly regarding statistical models. I also owe thanks to Dr. Ken Pollock for his input and comments on the early stages of this thesis.

I owe a great deal of thanks to the many people who helped me in Panama during field work, as well. I would especially like to thank Ricardo Moreno of Yaguará Panamá and Néstor Correa and Rafael Gómez of Asociación Panamericana para la Conservación for their collaboration and insight. This project would not have been possible without their support. I would also like to thank Ninon Meyer and Sergio Bermúdez for generously contributing data to our data fusion models; Smithsonian Tropical Research Institute and Smithsonian Institute Division of Mammals for their logistical support; and Roland Kays, Arielle Parsons, Lisa Gatens, Esther Langan, Nicole Edmison, Isaacs Rodrigues, and John Perrine for their invaluable help during camera deployments. Lastly, I would like to thank the many land owners whose support and hospitality made this project possible.

TABLE OF CONTENTS

LIST OF TABLES	vii
LIST OF FIGURES	ix
THESIS INTRODUCTION	1
LITERATURE CITED	3
CHAPTER 1	5
ABSTRACT	5
INTRODUCTION	6
METHODS	11
Movement Paths	13
Components of the Detection Process	14
Fine-scale Space Use	17
RESULTS	17
Movement Paths	18
Components of the Detection Process	18
Fine-scale Space Use	19
DISCUSSION	21
LITERATURE CITED	26
CHAPTER 2	39
ABSTRACT	39

INTRODUCTION	40
METHODS	42
Data Collection	42
Modeling	44
RESULTS	48
DISCUSSION	52
LITERATURE CITED	55
APPENDICES	72
Appendix A	73
Appendix B	75
Appendix C	77
Appendix D	78
Appendix E	80

LIST OF TABLES

CHAPTER 1

- Table 1. Definitions for components of detectability and their estimators. We formalized daily detection probability as a four-step process involving animal movement and camera efficacy. The probability of a camera detecting the target species involves the number of times per day that animals pass near the camera (\bar{N}), the probability that these animals will then pass close enough that the camera will take a picture (\bar{r}_c), and the probability of the camera sensing the animal and triggering fast enough to take an identifiable picture (r_t, r_p). We estimated these values from movement paths as described below, and used the components to estimate average daily detection probability for each species 31
- Table 2. Raw observed outcomes of animals passing camera traps. These observations were used to estimate the components of detectability described in Table 3. Camera outcomes are reported as the average proportion of camera visits that result in identifiable animal photographs, empty or unidentifiable photographs, or no photographs (no camera trigger). The associated 95% confidence intervals represent uncertainty in measuring these proportions based on the observed sample sizes (number of times cameras were passed). Reported outcomes for deer are based on a 10-day subset of the data due to the volume of detections. All other species considered all photographs captured during the 1-month sampling period 32
- Table 3. Estimated components of detectability. Components of detectability are defined as follows: average event rate (\bar{N}) is the average number of movement paths per day; average probability of camera visit given an event (\bar{r}_c) is the average proportion of cameras passed by an animal per movement path; probability of a camera trigger given a visit (r_t) is the proportion of all camera visits that resulted in a photograph; and probability of a photograph given a trigger (r_p) is the proportion of animal-triggered photographs that resulted in an identifiable animal photograph. P^* is daily detection probability for an individual camera empirically derived from these components, while P_{model} is daily detection probability estimated from the broad-scale Bayesian occupancy model. Deer detection components based on a 10-day subset of the data, while other species considered all photographs captured during the 1-month sampling period. 33

CHAPTER 2

Table 1. DIC results for top five crab-eating fox (*Cerdocyon thous*) data fusion models. Model covariates are defined as follows: ‘distance’=distance past c.2000 range boundary, ‘bait’=whether individual camera traps were baited/non-baited, ‘forest’=whether individual camera traps were deployed in forest/non-forest locations, ‘tree cover’=cell percent forest cover, ‘bc07’=cell annual temperature range (BIOCLIM-7), ‘bc16’=cell wet season precipitation (BIOCLIM-16), ‘+’ denotes an additive effect, and ‘.’ denotes no covariates. The top four models have competing support under DIC, but significantly outperform all other models. The top three models are nearly indistinguishable ($\Delta\text{DIC} < 5$), and the fourth model is competitive ($\Delta\text{DIC} < 10$) but less well-supported than the top three. The fitted models suggest that occupancy and GBIF records of crab-eating foxes become less common with westward distance into Panama. GBIF records may also occur less frequently in wetter, forested sites with pronounced seasonality, although the support for this is uncertain due to similarities in model DIC. In occupied sites, baited cameras deployed in non-forest locations detected crab-eating foxes more readily than non-baited cameras or cameras deployed in forested locations 61

Table 2. DIC results for top five coyote (*Canis latrans*) occupancy models. Covariates are defined as follows: ‘roadkill’= smoothed roadkill frequency (25-km radius) within cell, ‘tree cover’ = percent tree cover within cell, ‘bait’ = whether individual camera traps were baited/non-baited, ‘forest’ = whether individual camera traps were deployed in forest/non-forest habitat, ‘survey’ = whether individual camera traps were deployed in the 2015 survey or a recent collaborator survey. The top two models received indistinguishable support ($\Delta\text{DIC} < 5$), and the third model was competitive ($\Delta\text{DIC} < 10$) but less well-supported 62

APPENDIX A

Table 1. Results of time series analyses on animal detections 74

APPENDIX D

Table 1. Description of camera trap arrays in eastern Panama. “Site type” specifies whether a camera array was deployed within the agricultural corridor surrounding the Pan-American Highway (‘agricultural’) or an adjacent protected area (‘protected’). “Lat.” and “long.” gives the mean latitude and longitude of the array in decimal degrees (WGS84). “No. Cameras” gives the number of camera traps that were functioning at the end of the camera deployment and thus available for analysis, and “deployment” gives the average length of time that an individual camera was left in the field, in days 78

LIST OF FIGURES

CHAPTER 1

- Figure 1. Camera deployments in Schenck Forest and Umstead State Park. The fine-scale camera grid provided very high-resolution data from a single location near the center of Schenck Memorial Forest. A broad-scale camera survey was simultaneously conducted in the surrounding area and adjacent Umstead State Park in association with the eMammal citizen science monitoring project (Kays et al., 2016). 34
- Figure 2. Reconstructed raccoon movement path. Three cameras photographed a raccoon as it moved east over the grid at 2:59 AM on June 26, 2013. These photos are displayed chronologically to the left of the map. Within a minute, three more cameras took empty photographs in the direction that the animal was last seen moving. The timing and location of these photographs suggest that the raccoon triggered the cameras, but moved out of frame before a photograph could be taken. Inferred movement paths suggest that at least two other cameras were also visited, but not triggered 35
- Figure 3. Spatial and temporal variation in animal detections on the fine scale camera trapping grid. Cameras were placed at the southern end of each 10m grid cell and aimed northward. Uneven distribution of animal detections within the grid suggests fine-scale variation in animal space use. We were able to infer plausible biological reasons for this variation from behaviors observed in the photos. Some raccoon paths coincided with a small dry creek bed. Deer activity temporarily spiked in the center of the grid when a tulip poplar branch fell from the canopy during the first nine days of sampling. Coyote activity dramatically increased during the last few days, and animals were seen with food in their mouths, suggesting this was in relation to feeding event 36
- Figure 4. Proportion of cameras with detections at increasing deployment lengths. Coyotes and gray fox visits accumulated quickly during short bursts of activity, while deer and raccoons were steadily present throughout the study 37
- Figure 5. White-tailed deer (*Odocoileus virginianus*) detection rates at increasing distances from fallen tulip-poplar (*Liriodendron tulipifera*) branch. The branch fell on day 5, and detection rates remained high for the next two days until all leaves on the branch were consumed. No discernable increase was observed at adjacent cameras, even within 15 m 38

CHAPTER 2

Figure 1. Contemporary range expansion by coyotes (*Canis latrans*) and crab-eating foxes (*Cerdocyon thous*) in response to human disturbances. Both species have recently colonized agriculture-dominated landscapes in Panama, bringing them into contact for the first time. Continent-wide coyote range expansion based on historical records collected between 1850 and 2016 (Hody & Kays, *in prep*), and continent-wide crab-eating fox range expansion based on IUCN range estimates (NatureServe & IUCN, 2015, 2016). Range expansions in Panama based on the published literature (Reid 2006; Méndez-Carvajal and Moreno 2014) ... 63

Figure 2. Camera trap deployments in eastern Panama. Green area denotes forest cover as of 2000. Camera traps were placed in small arrays in an agricultural corridor along the Pan-American Highway during March – June 2015 through collaborations with local landowners. Camera traps were also placed in four adjacent protected areas during 2005 – 2015 by our collaborators Ricardo Moreno and Ninon Meyer 64

Figure 3. Diagram of data fusion model. Camera trap, roadkill, and GBIF data are analyzed together to estimate occupancy probability on a 7-km hexagonal grid. The data fusion model consists of two sub-models. Camera trap data acts as the primary data source, analyzed in an occupancy sub-model that treats grid cells as sites, and individual camera traps as spatial replicates within the cells. Roadkill data is integrated into this sub-model as a spatially-smoothed covariate. GBIF data acts as a secondary data source, analyzed in a presence-absence sub-model that also treats cells as sites. Here, crab-eating fox records act as presence data, and records of similar-sized non-arboreal terrestrial mammals are treated as pseudo-absences. Probability of occupancy (ψ) and probability of observing a crab-eating fox record in GBIF (p_{GBIF}) both include spatial random effects terms, defined using a multivariate CAR (MCAR) distribution that links the two sub-models. 65

Figure 4. Locations of camera deployments and detections of coyote and crab-eating foxes. Green area denotes forest cover as of 2000. Camera deployments spanned a 250-km long agricultural corridor along the Pan-American Highway and four protected forests across eastern Panama. Coyotes were only detected in the western portion of the study area, extending about 70 km west of the Panama Canal. Crab-eating foxes were detected in forested and agricultural habitats across eastern Panama 66

Figure 5. Daily distribution of coyote and crab-eating fox photographs during camera trap survey in spring 2015. Curves were fitted using circular kernel density estimators in the R-package ‘activity’ (Rowcliffe, 2016). Both species are nocturnal in eastern Panama, although coyotes appear to be active earlier in the evening and later in the morning than the foxes. General activity patterns of the crab-eating fox closely resemble those reported in South America, including the peak in activity just after dusk (Di Bitetti, Di Blanco, Pereira, Paviolo, & Pérez, 2009; D. W. Macdonald & Courtenay, 1996) 67

Figure 6. Parameter estimates for coyotes and crab-eating foxes in eastern Panama. Bars represent medians and 95% credible intervals based on the posterior distributions of the intercept values for occupancy and detection probability in the highest-ranked model for each species. Detection probability (p) is the probability of detecting a coyote or fox at an individual camera during a 21-day deployment, and occupancy probability (ψ) is the probability of a coyote or fox occupying a 7-km grid cell 68

Figure 7. Posterior distributions of covariate effects for top crab-eating fox model. Tree cover and distance from the c.2000 range boundary had negative effects on the probability of observing a GBIF record of a crab-eating fox (p_{GBIF}), although the effect of distance was modeled with high uncertainty. In the occupancy sub-model, forest cover had a negative effect on detection probability (p), and bait status had a positive effect on detection probability 69

Figure 8. Summary of mammal communities in disturbed habitats in eastern Panama. ‘Average detection rate’ is defined as the number of photo sequences per day, averaged across all camera traps. ‘Proportion of cameras’ denotes the proportion of all cameras that photographed the species at least once. Additional notes: (1) Domestic animals and humans are omitted from the figure, with the exception of domestic dogs and domestic cats. (2) Dog detections were only included if they occurred ≥ 5 minutes before or after detection of a human in order to better estimate the occurrence of free roaming dogs. Domestic cattle, horses, and sheep were not counted 70

Figure 9. Coyotes from in eastern Panama. Many of the coyotes that were photographed in eastern Panama had distinctly dog-like traits, including hound-like facial profiles, shortened tails, and variable dog-like pelage. These traits suggest that local coyote populations may be hybridizing with free roaming dogs 71

APPENDIX B

Figure 1. Summary of photographs, including putative missed detections. “Direct photograph” describes the number of unique images in which the species occurs within the frame. “Missed detection” describes the number of unique images where the animal triggered the camera, but moved out of the frame, making the image empty or unidentifiable. “Identified” describes the number of ‘no animal’ and ‘unidentifiable animal’ photographs that could be attributed to an animal species based on the 5-minute heuristic rule. Sample sizes (direct photographs and missed detections combined) are included alongside the species names 75

Figure 2. Assignment of "no animal" and "unknown animal" photographs. One “no animal” photograph was associated with a movement path of “unknown animal” photographs and was therefore reclassified as an “unknown animal” photograph 76

Figure 3. Trigger probability vs. body mass. Body masses based on those presented in Mammals of North America (Kays & Wilson, 2009). We observe a general increase in estimated trigger probability as the body mass of the species increases 77

APPENDIX D

Figure 1. Camera trap survey intensity in eastern Panama by grid cell. A lattice of 7-km hexagonal grid cells was superimposed across eastern Panama to facilitate data fusion models for crab-eating foxes and coyotes. Survey effort is defined here as the total number of trap-nights within individual grid cells, i.e. the number of days worth of data that were recorded within a grid cell. Total number of trap-nights increases with average deployment length and the number of cameras within a grid cell 79

APPENDIX E

Figure 1. Box plots of observed detection distances for humans at camera traps in forested and non-forested sites. Forest=1, non-forest=0. Detection distances were estimated in the field at the time of deployment by measuring the farthest distance at which the camera PIR sensor could reliably detect a walking camera trapper. Detection distances were similar in forest and non-forest sites on average, although detection distances in non-forest sites show a positive skew in their distribution. This indicates that some non-forest camera traps could detect animals further away than forested camera traps 80

INTRODUCTION

In the coming decades, land-use intensification and climate change are expected to dramatically impact global biodiversity, driving species range shifts, novel species interactions, and extinctions (Foley et al., 2005; Sala et al., 2000; Urban, Tewksbury, & Sheldon, 2012). This creates a major challenge for conservation programs and natural resource management agencies. To identify and manage threats to biodiversity in rapidly changing ecosystems, conservation programs increasingly require rapid, large-scale surveys of entire ecological communities. Such surveys have historically been difficult or cost-prohibitive for mammals and other mobile, elusive taxa, but passive sampling devices such as camera traps and microphone arrays have recently helped meet this demand.

Camera traps are a powerful and increasingly popular tool for studying terrestrial mammals. These devices allow researchers to rapidly collect large volumes of data on entire mammal communities, which can be used to address a wide array of ecological questions (Kays & Slauson, 2008). The prevalence of camera traps in peer-reviewed literature increased exponentially in the 1990s and 2000s (Rowcliffe & Carbone, 2008) and has continued to grow in recent years. However, as with any technology, camera traps have their limitations. Statistical analysis of camera trap data can be challenging, and many studies do not adequately consider the underlying detection process in their analyses (Burton et al., 2015).

I discuss some challenges and practical applications of camera traps here in two chapters. In chapter one, I use animal movement data from a fine-scale camera trap grid to

empirically describe the detection process underlying camera trap data. I relate our observations to the assumptions behind occupancy analysis (MacKenzie et al., 2002, 2006), a popular method for analyzing camera trap data (Burton et al., 2015). Additionally, I use our observations to provide some suggestions about data interpretation and analysis in future studies.

In chapter two, my collaborators and I use a large-scale camera trap survey to study an unfolding ecological scenario in eastern Panama. Coyotes (*Canis latrans*) and crab-eating foxes (*Cerdocyon thous*) are rapidly expanding their ranges in Central America, colonizing newly deforested areas alongside the Pan-American Highway (Méndez-Carvajal & Moreno, 2014; Reid, 2006; Tejera et al., 1999). Although these range expansions could have serious ecological consequences, very little information was known about either species in the area. Using camera traps and roadkill data, we document the current spatial distributions of the two species in Panama, describe their daily activity patterns, and investigate potential species interactions between the two. We also apply a suite of spatial data fusion models to examine existing hypotheses about why these species are expanding their ranges in Central America.

Camera traps present a valuable tool for conservation, allowing researchers to rapidly document how animal communities respond to changing environments. This technology opens new opportunities for in-depth ecological studies and informed, responsive management of biodiversity and natural resources. While some challenges remain, improved analyses and survey designs should facilitate exciting developments in this growing area of research.

REFERENCES

- Burton, A. C., Neilson, E., Moreira, D., Ladle, A., Steenweg, R., Fisher, J. T., ... Boutin, S. (2015). Wildlife camera trapping: A review and recommendations for linking surveys to ecological processes. *Journal of Applied Ecology*, 52(3), 675–685.
<http://doi.org/10.1111/1365-2664.12432>
- Kays, R. W., & Slauson, K. M. (2008). Remote Cameras. In R. A. Long, P. MacKay, W. J. Zielinski, & J. C. Ray (Eds.), *Noninvasive survey methods for carnivores* (pp. 110–140). Washington, DC, USA: Island Press.
- MacKenzie, D. I., Nichols, J. D., Lachman, G. B., Droege, S., Royle, J. A., & Langtimm, C. A. (2002). Estimating site occupancy rates when detection probabilities are less than one. *Ecology*, 83(8), 2248–2255.
- MacKenzie, D. I., Nichols, J. D., Royle, J. A., Pollock, K. H., Bailey, L. L., & Hines, J. E. (2006). *Occupancy estimation and modeling: Inferring patterns and dynamics of species occurrence* (1st ed.). Burlington, MA, USA: Elsevier Academic Press.
- Méndez-Carvajal, P., & Moreno, R. (2014). Mammalia, Carnivora, Canidae, *Canis latrans* (Say, 1893): Actual distribution in Panama. *Check List*, 10(2), 376–379.
- Reid, F. A. (2006). *A field guide to mammals of North America north of Mexico* (4th ed.). New York, NY, USA: Houghton Mifflin Company.

Rowcliffe, J. M., & Carbone, C. (2008). Surveys using camera traps: Are we looking to a brighter future? *Animal Conservation*, *11*(3), 185–186. <http://doi.org/10.1111/j.1469-1795.2008.00180.x>

Tejera, V. H., Araúz, J., León, V., Rodríguez, A. R., González, P., Bermúdez, S., & Moreno, R. (1999). Primer registro del zorro cangrejero, *Cerdocyon thous* (Carnivora: Canidae), Para Panamá. *Scientia*, *14*(2), 103–107.

CHAPTER 1

ABSTRACT

Passive sampling devices such as camera traps and microphones are increasingly used to study wildlife populations, but analytical questions remain about how to handle the imperfect detection of animals and how large of an area these data represent. Practitioners often assume that camera trap data represent animal space use within some larger area, and analyze it using occupancy analysis. However, camera traps only trigger and photograph animals that move through a small target window. Animals movement in and out of this small area clearly violates the closure assumption of occupancy analysis, but this has been judged acceptable by assuming that fine-scale animal movement is random and spatially homogeneous. Although violating these assumptions could bias occupancy estimates, they have not yet been tested against animal movement data. We deployed a grid of camera traps at 10-m intervals to map fine-scale animal movement paths and used these to empirically describe the detection process, quantify the cameras' abilities to detect four mammal species, and evaluate how animal activity at one camera location relates to a larger area. We found that fine-scale animal movements were nonrandom, causing detectability to be heterogeneous at fine spatial scales and also variable over time. Animal movements characterized by frequently-used movement corridors and localized hotspots of activity suggest that single camera sites were not accurate representations of animal activity in the larger grid area. One average camera run for one month detected 2.8 of the eight mammal species that used the 0.56 ha plot. Camera efficacy was lower than expected and varied between species. White-

tailed deer (*Odocoileus virginianus*) detected most reliably, being missed in only 14% of their passes by a camera (9% no trigger, 5% blank or poor image). Conversely, gray foxes (*Urocyon cinereoargenteus*) were the most difficult species to detect, being missed 71% of times they were presumed to walk by a camera (58% no trigger, 12% blank or poor image). The nonrandom movement of animals at fine scales we document means that single camera sites will serve as poor representatives of the larger area, emphasizing the need for arrays of multiple cameras. We conclude that occupancy analysis of camera trap data is not truly measuring the region around the camera is occupied, but is a measure of the probability use of a small plot in front of the camera. Similarly, detection probability describes the likelihood that the camera will actually trigger and capture a useful image of the animal when it is there. More research is needed to see if site level covariates can help predict the fine-scale nonrandom variation in animal movement and give our models more power to detect the larger scale trends in animal populations we need to understand to help manage and conserve them. Improved camera technology is also needed to increase the detectability of small and fast moving species.

INTRODUCTION

Global environmental changes have increased the need for large-scale biological surveys. Effective surveys of entire communities are particularly needed for mammals, which fill key roles in many ecosystems but are often at high risk for extinction and unevenly studied across taxa (Schipper et al., 2008). Most mammals are difficult to see or catch, so surveys are increasingly relying on noninvasive camera traps for terrestrial mammals

(Rowcliffe & Carbone, 2008) and acoustic monitoring for bats (Marques et al., 2013; O'Farrell & Gannon, 1999).

Statistical interpretation of passive monitoring data, however, can be challenging for most mammal species, because they cannot be identified as individuals. A recent literature review by Burton et al. (2015), emphasized that many studies do not adequately consider the theoretical relationships between camera trap detections (e.g., number of photographs) and the underlying processes driving detection (e.g., animal abundance, animal movement, and camera trap sensitivity), resulting in weakened inferences. They outline camera trap detections as a two-stage process involving: (1) the probability of an animal encountering a camera trap and (2) the probability of a camera photographing an animal if it passes within range of its field of view (Burton et al., 2015).

In a broader sense, this may be considered a sampling issue arising from the discrepancy between the desired spatial scale of ecological inference *vs.* the fine-scale nature of an individual camera trap. Camera traps are typically used in arrays to study large, mobile terrestrial mammals (Burton et al., 2015), often with the objective of monitoring broad-scale ecological processes such as population density, habitat use, or species interactions. Conversely, each individual camera monitors a small, stationary area of just a few square meters, extending in a cone in front of the camera's sensor (Hofmeester, Rowcliffe, & Jansen, 2016; Rowcliffe, Carbone, Jansen, Kays, & Kranstauber, 2011; Rowcliffe, Field, Turvey, & Carbone, 2008). Animal movement is consequently the factor linking camera trap data to ecological processes of interest.

The relationship between animal movement and detection probability is assumed in many analyses that are applied to camera trap data, although the strength of these assumptions vary dramatically among analyses and may not be explicitly stated. Movement assumptions are perhaps most clearly articulated in models for population density. Spatially-explicit capture-recapture (SECR) models assume that the probability of detecting an individual animal decreases with distance from its spatial center of activity (Efford, Dawson, & Borchers, 2009; Royle, Karanth, Gopalaswamy, & Kumar, 2009; Royle & Young, 2008). This is conceptually analogous to assuming that animals move in areas in the center of their home range more frequently than they do in areas near the periphery. Recent extensions of SECR models to unmarked and partially marked populations follow essentially the same assumptions (Chandler & Royle, 2013). Likewise, the random-encounter model (REM) proposed by Rowcliffe et al. (2008) explicitly relates the number of animal detections to population density and daily movement rate under the assumption that animals move randomly with respect to cameras (Rowcliffe et al., 2008; Rowcliffe, Kays, Carbone, & Jansen, 2013).

Occupancy models are among the most common analyses used with camera trap data to quantify animal abundance and habitat preference in unmarked animal species (Burton et al., 2015), but it still includes strong assumptions about animal movement that have not been well explored. In particular, animal movement affects the assumption of site closure, i.e. that surveyed locations remain either occupied or unoccupied throughout the entire sampling season. This is obviously violated when individual camera traps are treated as “sites” due to

the small area monitored in front of each camera trap (Efford & Dawson, 2012). To relax this, models assume that animals move in and out of sites at random, and that site use is stable across the sampling season (MacKenzie, 2005, 2012; MacKenzie et al., 2006).

Relaxing the closure assumption with this random-movement assumption comes with a price, as it changes the interpretation of both occupancy and detectability. If individual cameras are treated as sites, occupancy becomes “probability of use,” defined as the probability that an animal will use the site at least once during the study season (MacKenzie, 2005, 2012; MacKenzie et al., 2006). Note that ‘use’ does not imply that an animal is physically present at the site for the entirety of the sampling season. Rather, it implies that at least one animal periodically visits the site during sampling. In this sense, it may be helpful to think of occupied sites as locations that fall within at least one animal’s home range (Efford & Dawson, 2012). Likewise, detection probability takes on a new definition, and becomes the probability of an animal passing a camera (‘availability’) and the camera successfully photographing the animal during a replicate time period (MacKenzie, 2005, 2012), often a 1-, 5-, or 7-day interval.

The practicality and implications of the random-movement assumption remain largely untested for camera trap data. Efford and Dawson (2012) explored how the assumption affected true occupancy via theoretical models, and argued that occupancy in camera trap studies is a composite of population density and average home range size of the target species. This represents an important step forward, but it does not address the performance of occupancy models in estimating this parameter from camera trap data.

Avian point count studies provide some hypotheses. Hayes and Monfils (2015) used simulated data to test whether random animal movement within fixed home ranges affected the accuracy of occupancy estimates. They concluded that occupancy was positively biased and increased with home range size, but their results relied on a restrictive definition of true occupancy, which they defined as the physical presence of an animal (Latif, Ellis, & Amundson, 2016). Redefining occupancy as ‘use’ accounts for the supposed biases. Rota et al. (2009) offers a more comprehensive treatment of the subject, but defines animal movement as shifts in animals’ territories across longer periods of time (e.g., weeks) rather than random movement within established home ranges. They found that songbirds may frequently update their territories, and that these changes in space use can upwardly bias occupancy estimates and depress detection probability estimates. Extending these results to camera trap surveys, occupancy estimates might be biased high if animal space use changes while camera traps are deployed. This might occur at a broad spatial scale if animals relocate to new territories. It could also occur rapidly at a fine spatial scale if animals update habitat use within established territories.

However, no existing studies inform us whether such changes might be expected in a typical camera trapping survey. Likewise, no information is available about how well camera trap data represents animal space use in the larger area surrounding a camera trap, or the relative impacts of animal availability *versus* camera efficacy in determining detection probability. Answering these questions could greatly improve the design and interpretation of camera trap surveys involving occupancy.

Here, we empirically describe the detection process in a natural setting using a saturated array of camera traps placed systematically in 10m intervals. We use the camera trap data to reconstruct animal movement paths at a high resolution and used these to infer when and why cameras failed to detect passing animals. This allows us to observe the relative effects of animal movement and camera efficacy on species detection probability. Additionally, our data allow us to observe fine-scale variation in animal movement behavior and conceptually explore how representative single camera plots are to the larger area and how this may change through time.

METHODS

To simultaneously document animal movements and camera efficacy on a natural landscape, we deployed a fine-scale array of 56 newly purchased camera traps (Bushnell Trophy Cam HD, IR flash units) in Schenck Memorial Forest, North Carolina. Cameras were placed systematically at 10m intervals, forming a 70m by 80m rectangular grid that we operated continuously during June 13 – July 11, 2013 (Figure 1). Conceptually, this area represents a 0.5 ha plot of loblolly pine (*Pinus taeda*) forest nested within a much larger stand of managed loblolly pine, upland hardwood, and mixed forest habitat. The fine-scale data from this grid is complemented by a broader-scale dataset from Schenck Memorial Forest and adjacent Umstead State Park, collected during August – November, 2013 through the eMammal citizen science program (Kays et al., 2016; McShea, Forrester, Costello, He, & Kays, 2016).

We used similar settings at all cameras to ensure consistency across the grid. All cameras were set on trees at knee height, parallel to the ground and facing north. Each camera was set to a high trigger sensitivity with no quiet period between photographs, and timestamps were synchronized to the same clock. We neither baited the cameras nor attempted to place them along major habitat features. Instead, we documented potential sources of variation by recording the maximum distance at which cameras reliably detected a human walking (hereafter, detection distance) and noted the presence of putative game trails and understory vegetation at each camera location. While we recognize detection distances for humans may not match those of other mammals due to species-specific differences (Rowcliffe et al., 2011), it still provides a useful proxy for comparing variation in individual cameras' trigger sensitivities due to environmental factors such as vegetation complexity and visual obstructions.

Our intensive sampling effort provides unique insight into the process linking fine-scale animal movement to camera detections. Generally, an area this small would be treated as one camera "site," monitored by a single camera or pair of cameras. Here, we vastly increased survey effort, yielding over 1,430 trap-nights of continuous data from a single location. Animals moving across the grid generally passed in front of several cameras, allowing us to infer movement paths. We then used these reconstructed paths to infer how well the camera traps detected different mammal species.

Movement Paths

Every animal detection could be referenced to a specific place and time on the grid based on the camera ID and timestamp of the photograph. We used this information to reconstruct movement paths of unmarked animals moving across the grid (Figure 2), linking point detections into paths through a three-step process. First, we temporally grouped photographs into grid-level events using a simple heuristic rule chosen based on temporal autocorrelation in animal detections (Appendix A). If photographs of the same species occurred within 5 minutes of one another, we grouped them together into an event. Likewise, we considered photographs that contained no animals (i.e., empty photos) as putative missed detections if they occurred within 5 minutes of an animal photograph. Second, we ordered photographs chronologically within these grid-level events. Photographs were ordered primarily based on their timestamps, but we also considered the movement direction of animals within photos (e.g., whether the animal was heading east vs. west) in ambiguous cases where pictures occurred within the same minute or where multiple individuals visited the grid simultaneously. Finally, we constructed movement paths by connecting the shortest Euclidean distance between successive photographs. Events containing only one detection sometimes occurred, typically along the edge of the grid. In these cases, we assumed whichever path that intercepted the fewest camera traps. Reconstructed movement paths characterized fine-scale animal movement within the grid, and also provided a record of which cameras were visited and how cameras responded to passing animals.

Components of the Detection Process

We conceptualize detection as a four-step process involving both animal movement and camera efficacy. For a camera to photograph an individual animal, the animal must first (1) enter the general area (in this case the grid) and subsequently (2) pass in front of the camera. The animal must then (3) trip the camera's PIR trigger and (4) remain in frame long enough for the camera to take a picture.

This can be formalized using a modification of the Royle-Nichols model for abundance-induced heterogeneity in detection probability (Royle & Nichols, 2003):

$$p_i = 1 - [1 - (r_c * r_t * r_p)]^{N_i} \quad (1)$$

Here, p_i and is the probability of one camera detecting the target species on day i , and N_i is the number of times an individual animals entered the surrounding area (here, represented by the camera grid) on day i . We stress that the meaning of parameters here differ slightly from the original equation. Particularly, N_i in this case describes the daily number of visits to the grid, not necessarily the number of individual animals.

The remaining variables are a set of conditional probabilities:

$$r_c = \text{Pr}(\text{animal passes the camera} \mid \text{animal on the grid}) \quad (2)$$

$$r_t = \text{Pr}(\text{animal triggers the camera} \mid \text{animal on the grid, passes in front of camera}) \quad (3)$$

$$r_p = \text{Pr}(\text{animal is photographed} \mid \text{animal on the grid, passes camera, triggers camera}) \quad (4)$$

Our choice to divide N_i and r_c into two components is an arbitrary decision, which allows us to conceptualize space use on two spatial scales. Many practitioners assume that space use at neighboring camera locations is homogeneous and describe animal movement at

a camera trap and animal movement in a camera's immediate surroundings interchangeably (represented here by the camera and the grid). By dividing N_i and r_c , we are able to investigate the suitability of this assumption. It would be equally valid to describe the detection process solely in terms of the area directly in front of the camera. In this case, the 'grid' and 'camera' would describe the same area. The number of visits (N_i) would be smaller and $r_c = 1$, but the detection process would still be the result of both animal movement and cameras' abilities to detect passing animals. Occupancy, likewise, would retain the same definition as probability of use.

Using this framework, we analyzed the reconstructed animal movement paths to infer how well the camera traps detected different mammal species. We empirically estimated individual components of the detection process for each species as described in Table 1. To facilitate interpretation, we averaged daily number of visits to the grid (N_i) across days and probability of passing a camera (r_c) across cameras. For the average visit rate (\bar{N}), we averaged the number of movement paths recorded for each species across days. For the average probability of an animal passing an individual camera given a visit (\bar{r}_c), we calculated the average proportion of cameras that were passed per movement path, regardless of whether the camera took a picture. Similarly, we calculated probability of a camera triggering given a pass (r_t) as the proportion of all camera visits that resulted in a photograph, regardless of whether the animal was captured in the image. Lastly, we calculated probability of a camera photographing an animal given its trigger (r_p) as the proportion of animal-caused triggers that resulted in a photograph of the animal.

We estimated average daily detection probability (p^*) for each species by adding the observed components of detection into Equation 1. Since N_i is a count rather than rate, we could not directly insert \bar{N} into the equation. Instead, we generated 1000 random values of N_i from the Poisson distribution $Pois(\bar{N})$, calculated p_i for each sample, and averaged across these values to calculate p^* .

To check the validity of our approach, we compared our new empirically derived detection probability values from the small grid to conventional model-based approaches. Since camera spacing on our fine-scale grid was too small to allow conventional occupancy modeling, we fit single-species occupancy models to the broader-scale eMammal data (Figure 1) using WinBUGS v.1.4.3 (Lunn, Thomas, Best, & Spiegelhalter, 2000). Our primary interest in these models was not to estimate occupancy, but rather to estimate the expected range of values for the daily detection probability p_{model} in the Schenck Forest – Umstead State Park study area. We included a fixed effect of hiking trails and a random effect on detection probability p_{model} to account for spatial variation, and assumed a null model for occupancy probability ψ for each model (Appendix C). We estimated the distribution of p_{model} for off-trail cameras by predicting a value of p_{model} for each iteration of the Markov-chain Monte Carlo (MCMC). This approach accounts for both actual variation in detection probability and uncertainty in our parameter estimates. For each model, we ran three MCMC chains with a burn-in of 5,000 iterations, followed by a sample of 10,000 iterations with a thinning rate of 1. We assessed convergence using trace plots and Brooks-

Gelman-Rubin diagnostics for all parameters, treating $\hat{R} \leq 1.1$ as evidence of adequate convergence (Gelman et al., 2014).

Fine-scale Space Use

We summarized fine-scale space use patterns based on fine-scale detection rates (photo sequences per day at individual cameras) and animal behaviors caught on camera. Specifically, we described how detection rates changed across three 9-day intervals and relate these patterns to foraging behaviors and species-specific habitat features observed from the photographs. This section is predominantly descriptive, but illustrates potential sources of fine-scale heterogeneity across space and time. In doing so, we explore how well the random movement assumption applies to a real camera trap data, as well as potential implications for typical analyses.

RESULTS

Fifty-three out of 56 cameras ran continuously over a month, yielding over 1,430 trap-nights of data. Three cameras malfunctioned during the sampling period, and were therefore excluded from the analysis. Camera traps detected eight species of terrestrial mammals, not including humans and small rodents, with photographs of white-tailed deer (*Odocoileus virginianus*, hereafter ‘deer’) and humans occurring most frequently (Appendix B). Photographs containing “No Animal” were third most frequent type of detection (n=211). Interestingly, the majority of these photographs were associated with animal activity. About 63% (n=133) of these “empty” photo sequences occurred within 5 min of an

animal photograph. This is much higher than one might expect due to chance, as only 5% of the minutes in our total sample fell within 5 min of an identified animal photograph.

Movement Paths

Based on the number of detections for each species, we chose to focus our analyses on deer, northern raccoons (*Procyon lotor*, hereafter ‘raccoon’), coyotes (*Canis latrans*), and gray foxes (*Urocyon cinereoargenteus*). We analyzed a 10-day subset of data for deer due to a high volume of detections, but used the full dataset for the other three species. Two additional species, eastern gray squirrel (*Sciurus carolinensis*, hereafter ‘gray squirrel’) and Virginia opossum (*Didelphis virginiana*, hereafter ‘opossum’), were frequently detected but excluded from our study because their detections were too spatially and temporally disjointed to reliably infer movement paths. This might be due to the semi-arboreal nature of these species, which could allow them to traverse the grid above the cameras’ line of sight, or their smaller body size which would decrease detectability.

Components of the Detection Process

We used the reconstructed movement paths of the four focal species to investigate how reliably cameras photographed passing animals (Table 2). Generally, the cameras photographed animals more frequently than they failed to trigger and more frequently than they triggered late (i.e., producing “empty” images with no animals). Photographic success varied among species, from just 29% in gray foxes to 86% in deer. However, trigger failures (“no photos”) were always more common than failures due to rapid animal movement (“empty photos”).

Restructuring these values into components of detectability provided further insight into the detection process (Table 3). The probability of an animal encountering a camera (r_p) was consistently the smallest component of detectability, much smaller than trigger probability (r_t) and photo probability (r_p) within each of the four focal species. Trigger probability and photo probability were generally similar and comparatively large. Trigger probability showed the most between-species variation, probably increasing with body mass (Appendix B) and decreasing with animal speed (Glen, Cockburn, Nichols, Ekanayake, & Warburton, 2013; Rowcliffe et al., 2011).

The empirically-derived detection probabilities agreed with the model-based detection probabilities for all four species (Table 3). Although this does not necessarily ensure support for either method, the result is encouraging. The empirically-derived detection probabilities were sometimes toward the extreme ends of the fitted distributions, but always fell within the model-derived 95% Bayesian credible intervals (CIs). For example, empirically-derived deer detection probability was lower than the median model estimate, and empirically-derived coyote detection probability was higher than the median model estimate. However, both fell within the 95% CIs.

Fine-scale Space Use

We found evidence that animals used the fine-scale Schenck Forest grid unevenly in both space and time. In some cases, this variation aligned with species-specific foraging behaviors recorded in the camera trap pictures (Figure 3). For example, detection rates of raccoons were relatively high on the northeast corner of the grid, corresponding to a

frequently-used movement path along a dry creek bed, leading to a small stream north of the grid (Figure 1). Likewise, deer activity was unusually concentrated at a single station in the center of the grid during the first nine days of the study. Camera trap photos revealed that a tulip-poplar (*Liriodendron tulipifera*) branch had fallen from the canopy during a storm, providing the deer with a rich but short-lived foraging opportunity. Coyote activity was extremely clustered in both space and time, erupting in a series of east-west oriented paths on the south half of the grid for a few days towards the end of the study. Camera trap pictures showed individuals scent marking and carrying food items from an unseen location east of the grid, presumably related to a hunting event.

Interestingly, detections of different species exhibited different kinds of spatial heterogeneity. We observed repeated, parallel movement paths for both coyotes and raccoons, reminiscent of fine-scale functional corridors described for animal movement data (LaPoint, Gallery, Wikelski, & Kays, 2013). For these species, fine-scale space use was spatially heterogeneous but stable within these corridors for multiple days. However, the temporal clustering of coyote detections in the last nine days of the study (Figure 4) suggests that space use patterns can rapidly shift within the span of a typical camera trap deployment, potentially biasing model-based estimates of occupancy and detection probability (Rota et al., 2009). By comparison, deer detections were briefly concentrated at a randomly-occurring pocket of high-quality forage, but this event lasted only a few days and was extremely localized to the area immediately next to the branch itself (Figure 5). The chances of detecting such an event are likely very small; only one of the 53 functional cameras on our

grid detected any meaningful increase in deer activity. As such, we might regard this kind of heterogeneity as a relatively innocuous violation of typical occupancy assumptions, provided that foraging resources are not too patchily distributed.

DISCUSSION

Occupancy modeling is one of the most common analytical methods for camera trap studies but questions remain about how large of an area is represented by each camera, and the significance of violating assumptions that animal movement is random. Our unique fine-scale grid of cameras allowed us to map the movements of all animals using a small plot for the first time, test assumptions of random movement, quantify camera performance, and evaluate how representative one camera-site is of adjacent locations. Animals did not move randomly, resulting in high spatial and temporal heterogeneity, such that single cameras are not likely to represent the animal activity of the surrounding area well. Camera performance was also surprisingly poor, especially for smaller or faster moving species that frequently failed to trigger the camera, or moved out of frame before the image was taken. Low camera performance represents a technological challenge, but non-random space use is more problematic and could lead to biased occupancy estimates if poorly addressed.

Cameras frequently missed passing animals, with species-specific trends. For all four species that we studied, the probabilities of a camera triggering and then photographing an animal as it passed (r_t and r_p , respectively) were each less than 1. We found these results somewhat surprising, as we exclusively used new camera traps with fairly fast trigger speeds (0.4 s) in our study. Camera brands with slower triggers would miss more animals.

Individual components of detectability varied among species, following general patterns similar to those reported in previous studies (Glen et al., 2013; Hofmeester et al., 2016; Rowcliffe et al., 2011; Tobler, Carrillo-Percestequi, Leite Pitman, Mares, & Powell, 2008). Trigger probability (r_t) appeared to increase with the body mass of the target species (Appendix B). Likewise, the occurrence of “blank” images in which mammals moved out of the frame before a photograph could be taken suggests that faster-moving animals may be photographed less reliably than slow-moving animals.

However, despite these differences among species, the relative size of the components was consistent in all four species (Table 3). The probability of an animal encountering a camera given its presence on the grid (r_c) was consistently the smallest component in detectability. Probability of the camera triggering given an encounter (r_t) was consistently the second smallest component and varied the most among species, and probability of the camera photographing the animal given its trigger (r_p) was consistently the largest component. This seems to suggest that availability may be the factor which most greatly limits detection probability in camera trapping studies. We can explore this idea further by recalculating p^* under a hypothetical scenario where camera traps perfectly detected passing animals (i.e., $r_p=r_t=1$). Indeed, we find that daily detection probabilities would still be relatively small with ideal cameras, ranging from $p^* = 0.016$ for gray fox to $p^* = 0.171$ for deer. This does not imply that *variation* in detection probability is driven by animal space use, nor does it discount the importance of using high-quality camera traps and standardized equipment. Rather, it suggests that detection probability will likely be relatively small even

with perfect technology, and that meaningful improvements to p would require both improved technology and modified sampling designs. This is true not only for occupancy analysis, but also other analyses such as spatially-explicit capture-recapture.

Perhaps the most interesting and challenging observation from the Schenck Forest grid is the spatial variability in movements that we observed. Animal space use was generally heterogeneous, with critical differences between species. For raccoons and white-tailed deer, we observed biologically meaningful heterogeneity in fine-scale detections and movement paths. However, these fine-scale space use patterns appeared to be consistent throughout the duration of the study, and might have been biologically predictable. This stability through time suggests that occupancy models might be improved simply by adding random effects on detection probability and adding site-level covariates. While this comes at a computational cost and may indirectly reduce precision of occupancy estimates, model assumptions would more accurately reflect the structure of the data, providing more reliable estimates.

The coyote observations are more troubling. Although their fine-scale space use patterns were stable for a short period of time, these appeared to change over the 1-month duration of our study. This shift constitutes a nonrandom change in coyote space use patterns within a time period that would normally be used for a camera deployment, showing that the random movement assumption is not necessarily guaranteed for typical camera trap data. Here, camera-specific random effects and covariates are unlikely to improve estimates, and occupancy estimates may be artificially inflated unless open-population models are allowed

(Rota et al., 2009). Here, violations would be better addressed by restricting the length of camera deployments to a time period in which probability of use is unlikely to change (MacKenzie et al., 2006). Conventional animal tracking data may help identify time periods when broad-scale animal space use is consistent (e.g., consistent home ranges), but additional research is needed to explore whether fine-scale space use (e.g., paths and features within home ranges) typically change during camera trap studies.

In a general sense, our data suggests occupancy models can be useful in analyzing camera trap data, but that the reliability of these models will likely depend upon model choice and study design. Specifically, we recommend including random effects terms and fine-scale, species-specific habitat covariates on detection probability to offset spatial variation in animals' space use. Where possible, practitioners should also choose the length of their camera deployments to match temporal scales at which the home ranges of their target species is stable. Furthermore, detection probability may generally be low in camera trapping studies, and improved technologies (e.g., faster camera response times) and modified sampling designs (e.g., spatial replication) may be necessary to improve detection probabilities. Overall, camera trapping surveys and occupancy models represent valuable tools for studying species distributions, species interactions, and community structure, but models and study designs should be fine-tuned to match the biology of the target species or community.

Additionally, we conclude that occupancy analysis of camera trap data is not truly measuring the region around the camera is occupied, but is rather a measure of the

probability use of a small plot in front of the camera. Detection probability, likewise, describes the probability that an animal will cross through this small plot and that the camera will actually trigger and capture a useful image of the animal. Space use by animal can vary dramatically across small spatial distances, and recognizing a camera 'site' as the area directly in front of a camera has important implications for how data is collected and analyzed.

REFERENCES

- Burton, A. C., Neilson, E., Moreira, D., Ladle, A., Steenweg, R., Fisher, J. T., ... Boutin, S. (2015). Wildlife camera trapping: A review and recommendations for linking surveys to ecological processes. *Journal of Applied Ecology*, *52*(3), 675–685.
<http://doi.org/10.1111/1365-2664.12432>
- Chandler, R. B., & Royle, J. A. (2013). Spatially explicit models for inference about density in unmarked or partially marked populations. *Annals of Applied Statistics*, *7*(2), 936–954. <http://doi.org/10.1214/12-AOAS610>
- Efford, M. G., & Dawson, D. K. (2012). Occupancy in continuous habitat. *Ecosphere*, *3*(4), 32. <http://doi.org/10.1890/ES11-00308.1>
- Efford, M. G., Dawson, D. K., & Borchers, D. L. (2009). Population density estimated from locations of individuals on a passive detector array. *Ecology*, *90*(10), 2676–2682.
- Gelman, A., Carlin, J. B., Stern, H. S., Dunson, D. B., Vehtari, A., & Rubin, D. B. (2014). *Bayesian data analysis* (3rd ed.). Boca Raton, FL, USA: CRC Press.
- Glen, A. S., Cockburn, S., Nichols, M., Ekanayake, J., & Warburton, B. (2013). Optimising Camera Traps for Monitoring Small Mammals. *PLoS ONE*, *8*(6), e67940.
<http://doi.org/10.1371/journal.pone.0067940>
- Hayes, D. B., & Monfils, M. J. (2015). Occupancy modeling of bird point counts: Implications of mobile animals. *Journal of Wildlife Management*, *79*(8), 1361–1368.
<http://doi.org/10.1002/jwmg.943>

- Hofmeester, T. R., Rowcliffe, J. M., & Jansen, P. A. (2016). A simple method for estimating the effective detection distance of camera traps. *Remote Sensing in Ecology and Conservation*. <http://doi.org/10.1002/rse2.25>
- Kays, R., Parsons, A. W., Baker, M. C., Kalies, E. L., Forrester, T., Costello, R., ... McShea, W. J. (2016). Does hunting or hiking affect wildlife communities in protected areas? *Journal of Applied Ecology*. <http://doi.org/10.1111/1365-2664.12700>
- Kays, R. W., & Wilson, D. E. (2009). *Princeton field guides: Mammals of North America* (2nd ed.). Princeton, New Jersey, USA: Princeton University Press.
- LaPoint, S., Gallery, P., Wikelski, M., & Kays, R. (2013). Animal behavior, cost-based corridor models, and real corridors. *Landscape Ecology*, 28(8), 1615–1630. <http://doi.org/10.1007/s10980-013-9910-0>
- Latif, Q. S., Ellis, M. M., & Amundson, C. L. (2016). A broader definition of occupancy: Comment on Hayes and Monfils. *Journal of Wildlife Management*, 80(2), 192–194. <http://doi.org/10.1002/jwmg.1022>
- Lunn, D. J., Thomas, A., Best, N., & Spiegelhalter, D. (2000). WinBUGS – A Bayesian modelling framework: Concepts, structure, and extensibility. *Statistics and Computing*, 10, 325–337. <http://doi.org/10.1023/A:1008929526011>
- MacKenzie, D. I. (2005). What are the issues with presence-absence data for wildlife managers? *Journal of Wildlife Management*, 69(3), 849–860.

- MacKenzie, D. I. (2012). Study design and analysis options for demographic and species occurrence dynamics. In R. A. Gitzen, J. J. Millspaugh, A. B. Cooper, & D. S. Licht (Eds.), *Design and analysis of long-term ecological monitoring studies* (pp. 397–425). New York, NY, USA: Cambridge University Press.
<http://doi.org/10.1017/CBO9781139022422.024>
- MacKenzie, D. I., Nichols, J. D., Royle, J. A., Pollock, K. H., Bailey, L. L., & Hines, J. E. (2006). *Occupancy estimation and modeling: Inferring patterns and dynamics of species occurrence* (1st ed.). Burlington, MA, USA: Elsevier Academic Press.
- Marques, T. A., Thomas, L., Martin, S. W., Mellinger, D. K., Ward, J. A., Moretti, D. J., ... Tyack, P. L. (2013). Estimating animal population density using passive acoustics. *Biological Reviews*, 88(2), 287–309. <http://doi.org/10.1111/brv.12001>
- McShea, W. J., Forrester, T., Costello, R., He, Z., & Kays, R. (2016). Volunteer-run cameras as distributed sensors for macrosystem mammal research. *Landscape Ecology*, 31(1), 55–66. <http://doi.org/10.1007/s10980-015-0262-9>
- O'Farrell, M. J., & Gannon, W. L. (1999). A comparison of acoustic versus capture techniques for the inventory of bats. *Journal of Mammalogy*, 80(1), 24–30.
<http://doi.org/10.2307/1383204>
- Rota, C. T., Fletcher, R. J., Dorazio, R. M., & Betts, M. G. (2009). Occupancy estimation and the closure assumption. *Journal of Applied Ecology*, 46(6), 1173–1181.
<http://doi.org/10.1111/j.1365-2664.2009.01734.x>

- Rowcliffe, J. M., & Carbone, C. (2008). Surveys using camera traps: Are we looking to a brighter future? *Animal Conservation*, *11*(3), 185–186. <http://doi.org/10.1111/j.1469-1795.2008.00180.x>
- Rowcliffe, J. M., Carbone, C., Jansen, P. A., Kays, R., & Kranstauber, B. (2011). Quantifying the sensitivity of camera traps: An adapted distance sampling approach. *Methods in Ecology and Evolution*, *2*(5), 464–476. <http://doi.org/10.1111/j.2041-210X.2011.00094.x>
- Rowcliffe, J. M., Field, J., Turvey, S. T., & Carbone, C. (2008). Estimating animal density using camera traps without the need for individual recognition. *Journal of Applied Ecology*, *45*, 1228–1236. <http://doi.org/10.1111/j.1365-2664.2008.0>
- Rowcliffe, J. M., Kays, R., Carbone, C., & Jansen, P. A. (2013). Clarifying assumptions behind the estimation of animal density from camera trap rates. *Journal of Wildlife Management*, *77*(5), 876. <http://doi.org/10.1002/jwmg.533>
- Royle, J. A., Karanth, K. U., Gopalaswamy, A. M., & Kumar, N. S. (2009). Bayesian inference in camera trapping studies for a class of spatial capture-recapture models. *Ecology*, *90*(11), 3233–3244. <http://doi.org/10.1890/08-1481.1>
- Royle, J. A., & Nichols, J. D. (2003). Estimating abundance from repeated presence-absence data or point counts. *Ecology*, *84*(3), 777–790. [http://doi.org/10.1890/0012-9658\(2003\)084\[0777:EAFRPA\]2.0.CO;2](http://doi.org/10.1890/0012-9658(2003)084[0777:EAFRPA]2.0.CO;2)

- Royle, J. A., & Young, K. V. (2008). A hierarchical model for spatial capture-recapture data. *Ecology*, *89*(8), 2281–2289.
- SAS. (2015). JMP Pro (Version 12) [computer software]. Cary, NC, USA: SAS Institute Inc.
- Schipper, J., Chanson, J. S., Chiozza, F., Cox, N. A., Hoffmann, M., Katariya, V., ... Young, B. E. (2008). The status of the world's land and marine mammals: Diversity, threat, and knowledge. *Science*, *322*(5899), 225–230.
- Tobler, M. W., Carrillo-Percastegui, S. E., Leite Pitman, R., Mares, R., & Powell, G. (2008). An evaluation of camera traps for inventorying large- and medium-sized terrestrial rainforest mammals. *Animal Conservation*, *11*(3), 169–178.
<http://doi.org/10.1111/j.1469-1795.2008.00169.x>

Table 1. Definitions for components of detectability and their estimators. We formalized daily detection probability as a four-step process involving animal movement and camera efficacy. The probability of a camera detecting the target species involves the number of times per day that animals pass near the camera (\bar{N}), the probability that these animals will then pass close enough that the camera will take a picture (\bar{r}_c), and the probability of the camera sensing the animal and triggering fast enough to take an identifiable picture (r_t, r_p). We estimated these values from movement paths as described below, and used the components to estimate average daily detection probability for each species.

Parameter	Parameter Definition	Estimator Definition
\bar{N}	Average visit rate	Mean number of paths crossing the grid per day
\bar{r}_c	Pr(Pass Visit)	Mean number of cameras passed per path
r_t	Pr(Trigger Visit, Pass)	Proportion of passes resulting in any photograph
r_p	Pr(Photo Visit, Pass, Trigger)	Proportion of photographs that contain the animal

Table 2. Raw observed outcomes of animals passing camera traps. These observations were used to estimate the components of detectability described in Table 3. Camera outcomes are reported as the average proportion of camera visits that result in identifiable animal photographs, empty or unidentifiable photographs, or no photographs (no camera trigger). The associated 95% confidence intervals represent uncertainty in measuring these proportions based on the observed sample sizes (number of times cameras were passed). Reported outcomes for deer are based on a 10-day subset of the data due to the volume of detections. All other species considered all photographs captured during the 1-month sampling period.

Species	Proportion of Photo Outcomes			Sample Sizes	
	<i>Identifiable</i>	<i>Empty or Unclear</i>	<i>No Photos</i>	<i>Camera passes</i>	<i>Paths</i>
<i>Deer</i>	0.86 ± 0.06	0.05 ± 0.04	0.09 ± 0.05	123	21
<i>Raccoon</i>	0.47 ± 0.11	0.13 ± 0.08	0.39 ± 0.11	76	18
<i>Coyote</i>	0.57 ± 0.14	0.15 ± 0.10	0.28 ± 0.13	47	14
<i>Gray Fox</i>	0.29 ± 0.18	0.12 ± 0.13	0.58 ± 0.20	24	4

Table 3. Estimated components of detectability. Components of detectability are defined as follows: average event rate (\bar{N}) is the average number of movement paths per day; average probability of camera visit given an event (\bar{r}_c) is the average proportion of cameras passed by an animal per movement path; probability of a camera trigger given a visit (r_t) is the proportion of all camera visits that resulted in a photograph; and probability of a photograph given a trigger (r_p) is the proportion of animal-triggered photographs that resulted in an identifiable animal photograph. P^* is daily detection probability for an individual camera empirically derived from these components, while P_{model} is daily detection probability estimated from the broad-scale Bayesian occupancy model. Deer detection components based on a 10-day subset of the data, while other species considered all photographs captured during the 1-month sampling period.

<i>Species</i>	\bar{N}	\bar{r}_c	r_t	r_p	p^*	p_{model} (<i>Median, 95% CI</i>)
<i>Deer</i>	1.70	0.11	0.91	0.95	0.153	0.443 (0.068 – 0.896)
<i>Raccoon</i>	0.67	0.08	0.61	0.78	0.025	0.020 (0.002 – 0.158)
<i>Coyote</i>	0.52	0.06	0.72	0.79	0.018	0.005 (0.001 – 0.027)
<i>Gray Fox</i>	0.15	0.11	0.42	0.70	0.005	0.010 (0.001 – 0.088)

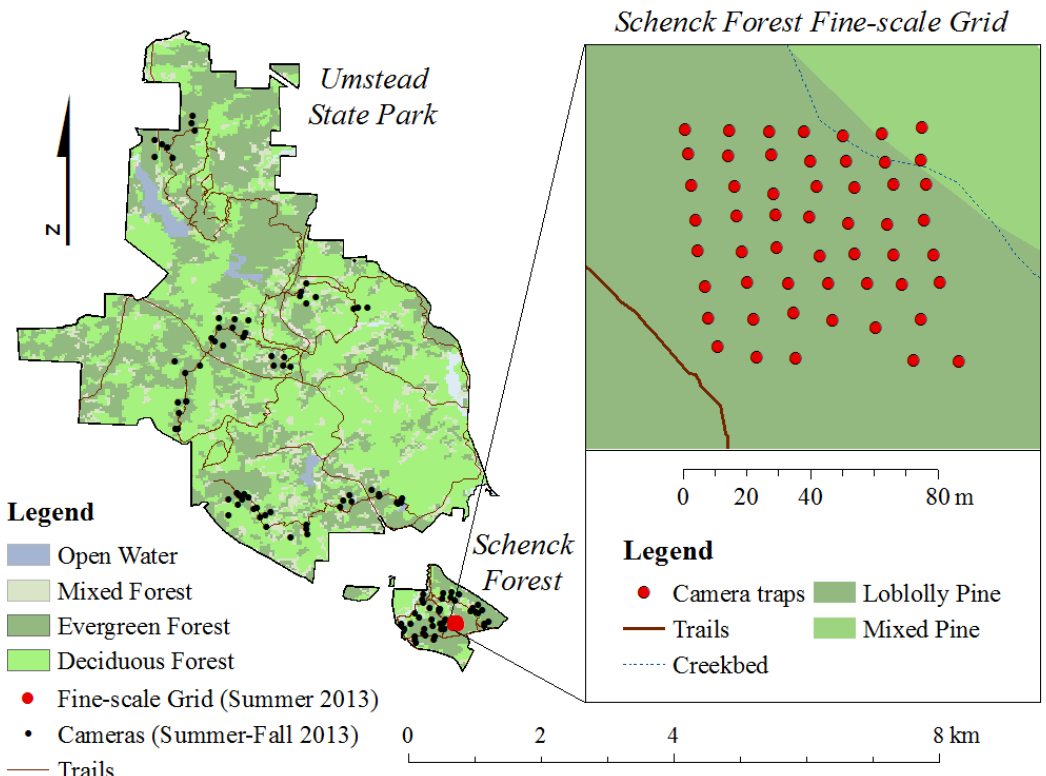


Figure 1. Camera deployments in Schenck Forest and Umstead State Park. The fine-scale camera grid provided very high-resolution data from a single location near the center of Schenck Memorial Forest. A broad-scale camera survey was simultaneously conducted in the surrounding area and adjacent Umstead State Park in association with the eMammal citizen science monitoring project (Kays et al., 2016).

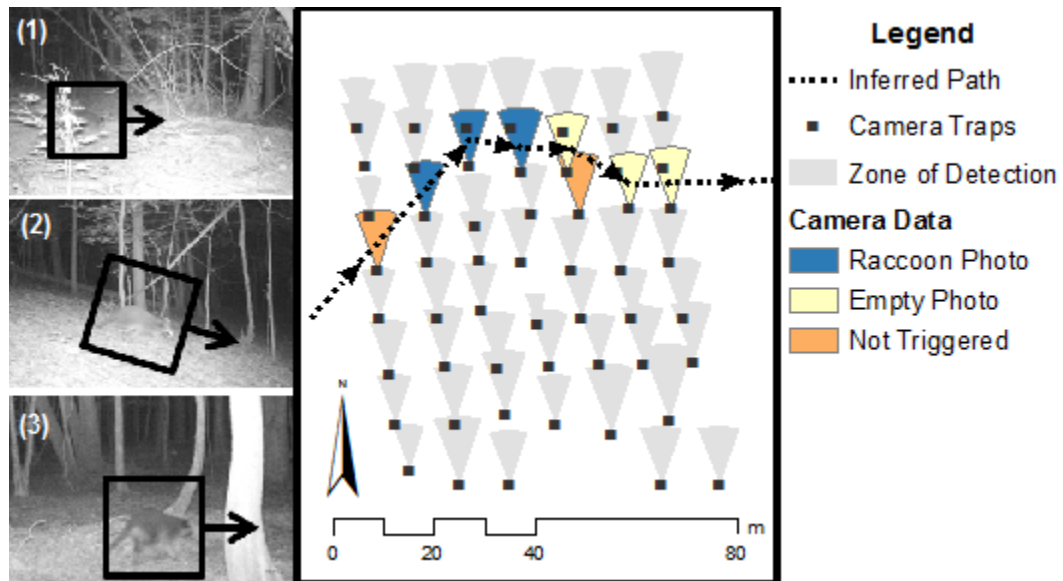


Figure 2. Reconstructed raccoon movement path. Three cameras photographed a raccoon as it moved east over the grid at 2:59 AM on June 26, 2013. These photos are displayed chronologically to the left of the map. Within a minute, three more cameras took empty photographs in the direction that the animal was last seen moving. The timing and location of these photographs suggest that the raccoon triggered the cameras, but moved out of frame before a photograph could be taken. Inferred movement paths suggest that at least two other cameras were also visited, but not triggered.

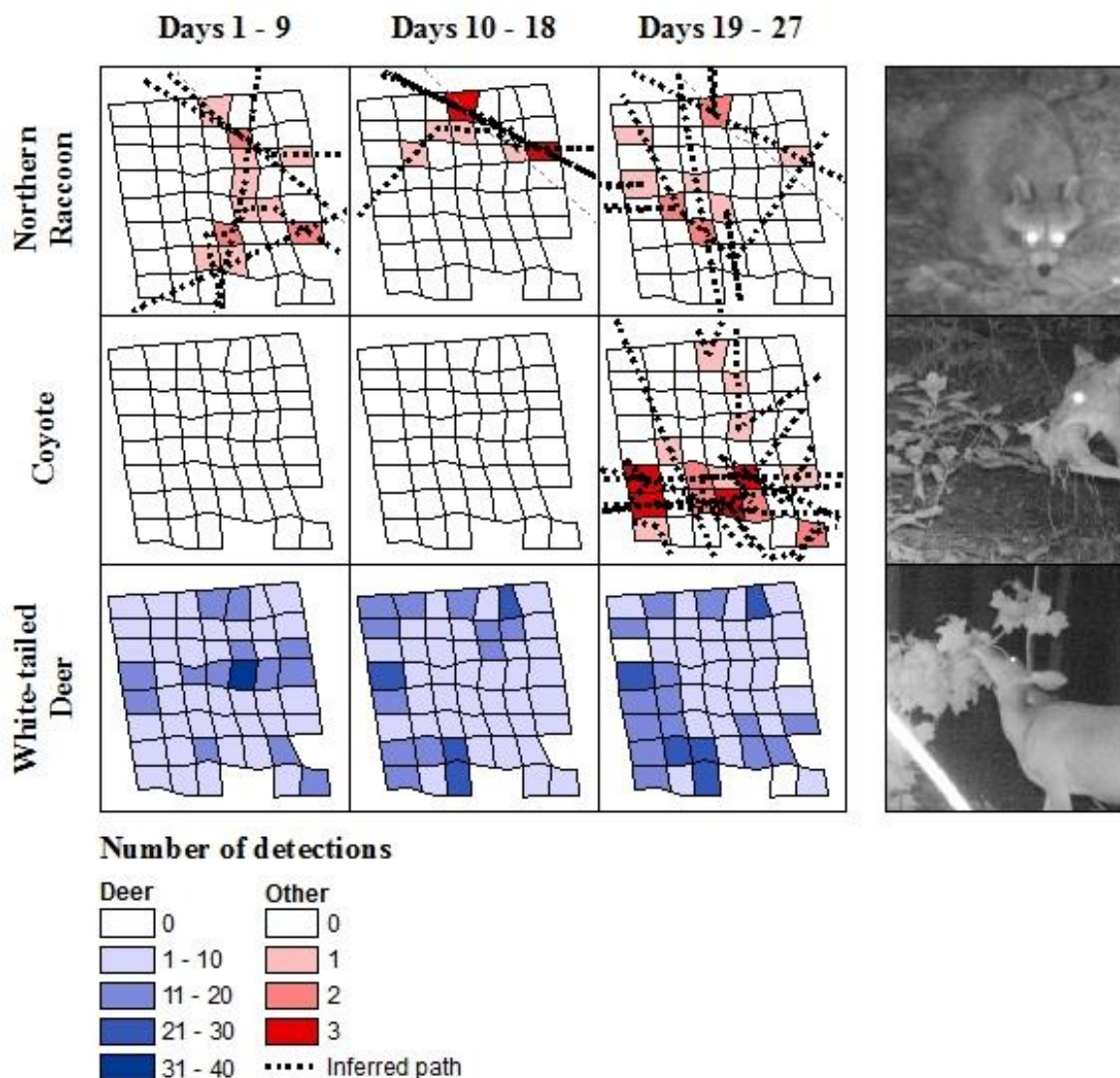


Figure 3. Spatial and temporal variation in animal detections on the fine scale camera trapping grid. Cameras were placed at the southern end of each 10m grid cell and aimed northward. Uneven distribution of animal detections within the grid suggests fine-scale variation in animal space use. We were able to infer plausible biological reasons for this variation from behaviors observed in the photos. Some raccoon paths coincided with a small dry creek bed. Deer activity temporarily spiked in the center of the grid when a tulip poplar branch fell from the canopy during the first nine days of sampling. Coyote activity dramatically increased during the last few days, and animals were seen with food in their mouths, suggesting this was in relation to feeding event.

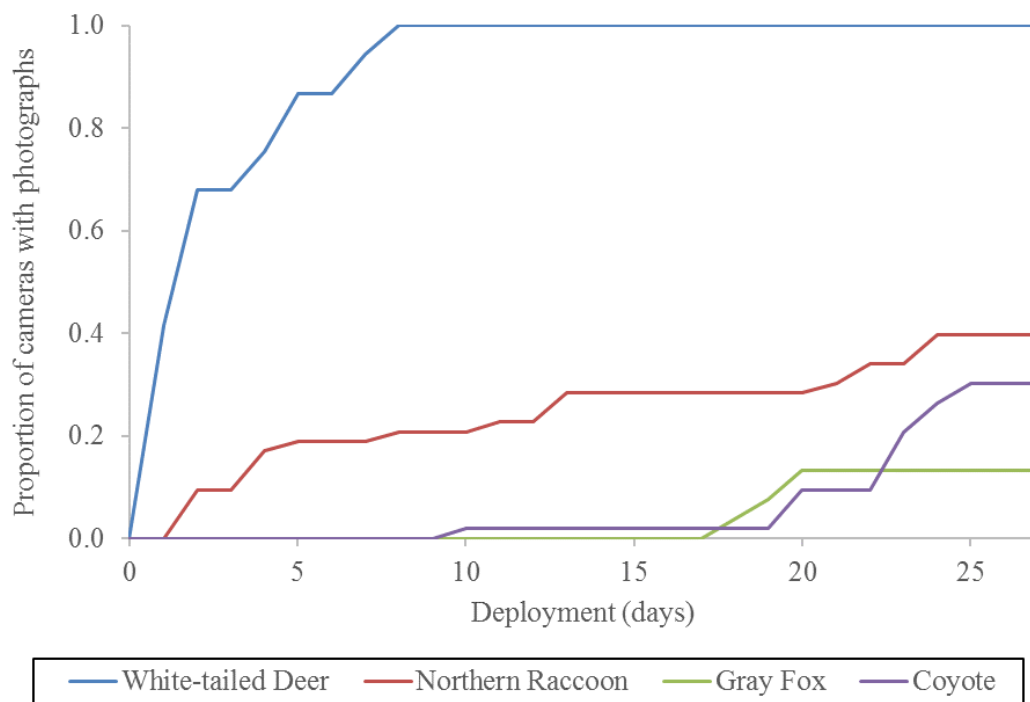


Figure 4. Proportion of cameras with detections at increasing deployment lengths. Coyotes and gray fox visits accumulated quickly during short bursts of activity, while deer and raccoons were steadily present throughout the study.

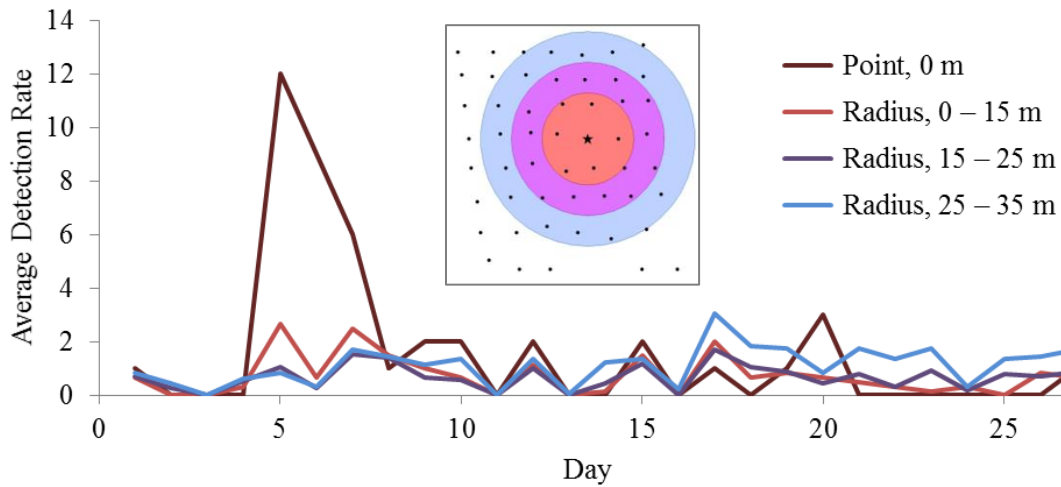


Figure 5. White-tailed deer (*Odocoileus virginianus*) detection rates at increasing distances from fallen tulip-poplar (*Liriodendron tulipifera*) branch. The branch fell on day 5, and detection rates remained high for the next two days until all leaves on the branch were consumed. No discernable increase was observed at adjacent cameras, even within 15 m.

CHAPTER 2

ABSTRACT

Coyotes (*Canis latrans*) and crab-eating foxes (*Cerdocyon thous*) are highly-adaptable canids that have rapidly expanded their ranges in recent decades. Although these species have always lived on separate continents, both have recently colonized Central America, and their expanding populations appear to be approaching each other in eastern Panama. We used camera traps study this novel zone of contact monitoring 105 locations human-modified landscapes and 98 locations from nearby protected forests. We also compiled a database of auxiliary occurrence records from the region including museum specimens and roadkill records. We estimated distribution patterns by modeling these data in a spatial data fusion framework, fitting the different data sources with separate but spatially correlated hierarchical models. We found the range of coyotes and crab-eating foxes now overlaps in the area between the Panama Canal and Lago Bayano. Despite this broad scale overlap, however, the two species were never detected within the same camera array, suggesting fine scale spatial avoidance. Both species were primarily nocturnal. Our models suggest different, yet overlapping habitat use for the two species in Panama. Coyotes and foxes both appear to use open habitats, but possibly to different degrees. The limited range overlap of coyotes and foxes in our study restrict our inference on competition between the two species. However, the fact that we never found both species at the same camera array suggests competition could be important, and might limit future range expansion. Our models suggest that the great forests of Darién will still pose a significant barrier for coyotes,

and might prevent them from reaching South America, which otherwise has apparently suitable habitat.

INTRODUCTION

The closure of Panamanian Isthmus around 3-4 million years ago facilitated an unprecedented exchange of fauna between North and South America, known as the Great American Biotic Interchange (Leigh, O’Dea, & Vermeij, 2014; Marshall, Webb, Sepkoski, & Raup, 1982; Simpson, 1980; Wallace, 1876). These species invasions dramatically affected both regions, and is one of the most famous biogeographic events in history (Leigh et al., 2014; MacFadden, 2006). Central America today continues to form an important linkage for broad ranging species such as the jaguar and tapir, although there is concern that deforestation could sever this link (Olsoy et al., 2016; Schank et al., 2015). Between 1990 and 2015, Central American countries lost a quarter of their tropical forests, with Panama alone losing some 423,000 hectares (8.4%) of its forest cover during this period (FAO, 2015).

As deforestation extends across the Panamanian Isthmus, the land bridge becomes less suitable for forest-dwelling species but could also become increasingly permeable to disturbance-adapted species that can thrive in expanding urban and agricultural habitats. In this regard, the deforestation of Panama could be creating a new corridor between non-forested landscapes in North and South America. This could facilitate a new era of intercontinental biotic interchange, especially generalist species able to thrive near development, with unknown ecological consequences for both continents.

At least two mammal species have already begun to colonize this new corridor: the coyote (*Canis latrans*) from North America and the crab-eating fox (*Cerdocyon thous*) from South America. Both species are highly adaptable mid-sized canids that readily exploit human-disturbed ecosystems (David W. Macdonald & Sillero-Zubiri, 2004), allowing them to achieve nearly continent-wide distributions in their original hemispheres (Figure 1). During the twentieth century, the coyote dramatically expanded its range across North America due to deforestation, removal of large predators, and hybridization with gray wolves (*Canis lupus*) and domestic dogs (*Canis familiaris*) (Kays, Curtis, & Kirchman, 2010; Moore & Parker, 1992; Parker, 1995). Coyotes simultaneously spread southward from Mexico and Guatemala, reaching Costa Rica by the 1960s (Vaughan, 1983) and western Panama by the 1980s (Méndez, Delgado, & Miranda, 1981). Likewise, crab-eating foxes recently expanded their geographic range in South America by exploiting human disturbances (Cuervo Díaz, Hernández-Camacho, & Cadena, 1986). Observations of foxes in new parts of northern South America and genetic evidence from Brazilian populations suggests that expansion has continued at both the northern and southern extremes of their current distribution (Hadik-Barkoczy, 2013; Ramírez-Chaves & Pérez, 2015; Tchaicka, Eizirik, De Oliveira, Cândido, & Freitas, 2007; Tejera et al., 1999; Thoisy, Vergara, Silvestro, & Vasconcelos, 2013).

Just within the past decade both species colonized eastern Panama (Figure 1). Coyotes reached the Panama Canal as recently as the early 2000s (Springer et al., 2012) and successfully crossed eastward across this barrier by 2013 (Méndez-Carvajal & Moreno, 2014). At the same time, crab-eating foxes colonized eastern Panama through the Darién

Gap (Tejera et al., 1999), a heavily forested area along the Panama-Colombia border, and expanded halfway to the Panama Canal within just five years (Reid, 2006). The two species now co-occur in the same region for the first time ever, prompting several questions about how the two species may interact, whether they will expand further, and how they may affect local wildlife.

We investigated the current distribution and broad-scale habitat associations of these two species using camera traps and opportunistic roadkill surveys, as well as occurrence records published by the Global Biodiversity Information Facility (GBIF). Using a novel data fusion approach, we jointly analyze all available data to estimate occupancy probability for coyotes and crab-eating foxes across Panama. We also summarize detections of other wildlife species in these areas and discuss potential further expansion of the two species in Panama.

METHODS

Data Collection

We conducted a broad-scale survey for canids in eastern Panama using camera traps and opportunistic roadkill surveys during March – June 2015. We coordinated with local landowners to deploy small arrays of camera traps throughout a 250 km agriculture-dominated corridor along the Pan-American Highway (Figure 2). To promote spatial independence, we used a minimum spacing of 7.5 km between arrays and 250 m between individual cameras (Reconyx Hyperfire and Ultrafire). The 7.5 km spacing between arrays was chosen based on reported home ranges for coyotes and crab-eating foxes in similar

habitats. Locations where we placed camera arrays (henceforth, “sites”) generally contained a combination of cattle fields, remnant patches of tropical forest, and small plantings of crops such as plantains. Two sites contained large non-native tree plantings (oil palm *Elaeis guineensis* and teak *Tectona grandis*) in addition to these cover types. At each site, we deployed half of the cameras in open fields and half in remnant forests to sample major cover types equally. Furthermore, we baited a subset of cameras at each site with perforated cans of fish, staked to the ground in front of the camera. Cameras were deployed for at least three weeks each site, although some deployments lasted longer due to logistical difficulties in accessing remote locations. In total, we collected 3,464 trap-nights of data from 105 camera locations in fragmented habitats between the Panama Canal and the end of the Pan-American Highway in Yaviza, Darién Province. While driving between sites, we also scanned the road for coyote and crab-eating fox roadkill. In cases where we observed carcasses, we photographed the animal, noted its surroundings and position on the road, and recorded its location using a handheld GPS device.

We also included camera trap data collected by Ricardo Moreno and Ninon Meyer between 2005 and 2015 from four protected areas into the analysis (Figure 2). This dataset provides inference about the large intact tropical forests adjacent to our study area, specifically those in Soberania National Park, Guna Yala, and Darién National Park. Camera deployments by our collaborators differed from ours in some regards, which we address in our models. Deployment lengths were generally longer than those conducted on private

lands, no cameras were baited, and camera models differed from those used in our study. In total, this dataset included a total of 6,984 trap-nights of data from 98 camera locations.

Additionally, we compiled georeferenced records for both species in Panama and neighboring countries from the Global Biodiversity Information Facility (GBIF), peer-reviewed literature, and roadkill records from collaborators. We took precautions to ensure that GBIF records were spatially and temporally relevant. GBIF data were filtered to only include georeferenced records collected after 2000 in Costa Rica, Panama, Colombia, Venezuela, or Ecuador. Furthermore, we downloaded records from mid- to large-sized terrestrial mammals from the same area and time period to provide some indication of spatial survey effort.

Modeling

We estimated broad-scale occupancy patterns for crab-eating foxes across eastern Panama by jointly analyzing all available information in a spatial data fusion framework (Pacifi et al., 2016). Our data fusion model consisted of two sub-models, linked through a correlated random effects term (Figure 3). Specifically, the model included: (1) an occupancy sub-model for the camera trap data, (2) a presence-pseudoabsence sub-model for the GBIF occurrence data. For the correlated random effects term, we defined ‘sites’ the same way for both sub-models by superimposing a 7 km hexagonal grid across the study area (Appendix D). We then linked cell-specific occupancy probability (ψ) from the first sub-model to cell-specific probability of a GBIF record (p_{GBIF}) from the second sub-model within each grid cell using a shared multivariate CAR (MCAR) term.

While statistically complex, this ‘correlation model’ formalizes an intuitive hypothesis (Pacifici et al., 2016). Camera trap and GBIF data are not interchangeable, but we might expect them to share similar spatial patterns. For example, sites that are more likely to have foxes (higher occupancy probability, ψ) might also have more GBIF occurrence records (higher probability of a GBIF record, p_{GBIF}). Here, the MCAR term would allow high correlation between the sub-models, and the GBIF data would indirectly inform occupancy estimates. Conversely, the model can also allow for low correlation between sub-models if the data are unrelated, in which case occupancy estimates draw almost exclusively from the camera trap data (Pacifici et al., 2016). We also incorporated roadkill data into the model. Roadkill frequency was spatially smoothed at a 25 km radius and included as a covariate in the occupancy sub-model. The covariate approach is less explicit than the correlation approach used with the GBIF data, but still shares valuable information across datasets (Pacifici et al., 2016).

Due to difficulties getting the data fusion model to run for the coyote data, we used a more conventional approach. We applied a single-season, single-species occupancy model to the camera trap data (MacKenzie et al., 2002, 2006), again treating 7-km hexagonal grid cells as sites and individual camera traps as replicate spatial samples within the grid cells. Roadkill data were included as a smoothed covariate (25 km radius), but the GBIF sub-model was not included in the analysis.

For both species, we developed *a priori* models based on their known biology in their native ranges. We developed occupancy and presence covariates for percent tree cover,

annual temperature range (BIO-7, hereafter “seasonality”), and wet season precipitation (BIO-16) based on bioclimatic variables and high-resolution land use data (Hansen et al., 2013; Hijmans, Cameron, Parra, Jones, & Jarvis, 2005). Coyotes tend to prefer open habitats in North America (David W. Macdonald & Sillero-Zubiri, 2004), and the species was historically restricted to arid and temperate conditions. Thus, we expect coyote occupancy to be higher in open, drier sites. The crab-eating fox favors copses, wooded savannahs, and disturbed sites on its native range, but avoids flooding areas (D. W. Macdonald & Courtenay, 1996; David W. Macdonald & Sillero-Zubiri, 2004). We predict fox occupancy to be higher in open, drier, less seasonal sites, while acknowledging that its relationship with forest cover may be nonlinear due to their preferential use of forest edges and partially wooded sites. Furthermore, we included covariates for roadkill and distance from the species’ range boundaries *circa* 2000 to incorporate the roadkill data and account for the fact that occupancy may be initially low and less variable in recently-colonized areas (Yackulic, Nichols, Reid, & Der, 2015).

We considered three covariates for detection probability in the occupancy sub-model. These included bait status and local forest cover, with the assumption that baited cameras and cameras in open sites may detect animals more easily than unbaited cameras and cameras in forested locations. Note that forest covariates for detection probability refer to local cover at the scale of an individual camera trap, contrasting the broad scale of the occupancy forest covariate. Survey ID (whether cameras were deployed in 2015 or earlier) was also included to account for potential differences between the surveys, such as camera model. We adjusted

detection probability to account for the deployment lengths of different cameras, but this was not addressed via covariates. Rather, we scaled detection probability using the equation: $p_{\text{total}} = 1 - (1 - p_{\text{daily}})^N$, where p_{total} is detection probability for the full deployment, p_{daily} is detection probability for a 1-day deployment, and N is the number of days that the camera was deployed.

We developed and tested all models in WinBUGS v.1.4.3 (Lunn et al., 2000). Prior distributions for all intercepts and covariates were set to $N(\mu=0, \sigma^2=100)$, and initial values were randomly drawn from the prior distributions. Each model was run with three chains for at least 80,000 MCMC iterations, discarding the first 40,000 as burn-in.

Models were ranked based on the Deviance Information Criterion (DIC), a Bayesian measure of relative model fit similar to AIC (Spiegelhalter, Best, Carlin, & van der Linde, 2002). We considered models to be virtually equivalent if the difference between their DIC values was less than 5, and competitive if the difference in the DIC values was less than 10. For the crab-eating fox data fusion model, selection was a three-step process. First, we selected a top model for detection probability (p) in the occupancy sub-model by holding occupancy probability (ψ) and presence probability (p_{GBIF}) constant. We then selected a top model for presence probability (p_{GBIF}) by holding occupancy probability (ψ) constant and using the top model for detection probability (p). Finally, we selected a top model for occupancy probability (ψ). For the coyote occupancy model, selection was a two-step process. We first determined the top detection model, then applied it to determine the top occupancy model.

Our modeling approach allows us to consider data from multiple sources, while also acknowledging differences in how they were collected and sampled. This is an important step forward from previous techniques, as it allows us to describe the data more accurately and quantify uncertainty in broad-scale space use patterns.

RESULTS

Our results confirm that coyotes and crab-eating foxes now overlap in eastern Panama, marking the first-ever interaction between the two species. Raw observations suggest high temporal overlap in their daily activity patterns, and suggest possible spatial avoidance of the two species. However, more data is needed to confirm these possible behaviors. Our analysis generally favored models with few occupancy covariates due to the small number of coyote and fox detections, but provide some insights into the species' biology in Panama. Distance from previous range boundaries emerged as an important factor on occupancy for foxes, suggesting that they still in the early stages of colonizing eastern Panama, which may mask occupancy patterns in the area (Yackulic et al., 2015).

The raw spatial distribution of coyote and fox detections reveal that the two species co-occur in a large area between the Panama Canal to Chepo in the Panamá District (Figure 4). Crab-eating foxes appear to have colonized eastern Panama more quickly, with detections across our study area. Conversely, our coyote detections coincided almost identically with those reported by Méndez-Carvajal and Moreno (2014), although with improved spatial detail. We detected the two species in extremely close proximity, within 8 km near Chepo, Panamá. Interestingly we did not detect the two species together at any site,

despite finding them in very similar sites and habitats. This may suggest spatial avoidance between the two species, although the sparseness of coyote and fox detections make it difficult to test this hypothesis. Timing of coyote and fox photographs from our camera trap survey suggest large temporal overlap in the species' activity patterns during the early evening and night, emphasizing the potential importance of spatial segregation for these species (Figure 5).

Model selection favored relatively simple models, likely due to the low number of coyote and fox detections in each data set. Top ranking models closely competed under DIC for coyotes and crab-eating foxes, but DIC consistently favored few or no covariates on occupancy probability (ψ). For the top-ranked crab-eating fox models, occupancy was either constant or included a distance effect, with occupancy probability decreasing with westward distance into Panama (Table 1). For the top-ranked coyote models, roadkill frequency was included as a covariate (Table 2). However, the modeled relationship was surprisingly negative. Since coyote roadkills were all documented near densely urban areas around Panama City, this may be a spurious relationship indicating avoidance of urban sites, or the proximity of Panama City to the densely-forested Soberania National Park.

Covariates for detection probability (p) and GBIF presence probability (p_{GBIF}) were consistently favored in the models. Detection probability covariates were similar for the two species. Bait response and local forest cover emerged as important covariates for both coyotes and crab-eating foxes (Table 1, Table 2). As predicted, detection probability was significantly higher at baited cameras *vs.* non-baited cameras, and significantly lower at

cameras placed in forests *vs.* open areas. This trend was consistent across all fitted models for both species. Here, the negative effect of forest cover may be biologically meaningful. For spatial replicates, detection probability is a combination of probability of using a site and being detected. Higher detection probability in non-forest locations could indicate that camera traps detect animals at greater distances due to the lack of visual obstructions (Hofmeester et al., 2016), or it could reflect preferential fine-scale habitat selection for non-forest locations. Detection distances were similar between forest and non-forest sites in our study (Appendix E), but either explanation is plausible. GBIF presence probability (p_{GBIF}) in the crab-eating fox model consistently included a distance effect and a possible negative relationship with percent tree cover. The significance of this effect is unclear due to the similar performances among the top four models (Table 1), but may suggest broad-scale avoidance of forested sites in areas where the species is already established.

Detection probability was very low for both coyotes and crab-eating foxes, and occupancy estimates had relatively low precision due to the small number of coyote and fox detections overall (Figure 6). This may also explain the preference for less complex models, favoring fewer covariates on occupancy probability. In this respect, improving detection probability and overall number of detections may be an important step in future attempts to study and monitor both species in eastern Panama. Baiting significantly increased detection probability in coyotes and crab-eating foxes (Figure 7). Although this could interfere with studies on fine-scale habitat selection (i.e., camera traps as ‘sites’) (Efford & Dawson, 2012), it may be suitable for surveys targeting broad-scale spatial patterns (Gerber, Karpanty, &

Kelly, 2012). Additional research is needed to assess its suitability if widely applied in broad-scale occupancy studies, but it could represent a valuable tool in studying canid range expansion if fine-scale habitat use is not a main process of interest.

We documented several other mammal species in addition to coyotes and crab-eating foxes. Not surprisingly, the species that we most frequently detected on agricultural sites were those generally associated with fragmented and exploited forests (Meyer et al., 2015) (Figure 8). Notably, the black-eared opossum (*Didelphis marsupialis*), nine-banded armadillo (*Dasypus novemcinctus*), and white-nosed coati (*Nasua narica*) were photographed frequently at a large proportion of camera locations. However, we also detected several rare and threatened species in the agricultural landscape, including the giant anteater (*Myrmecophaga tridactyla*), jaguar (*Panthera onca*), greater grison (*Galictis vittata*), and naked-tailed armadillo (*Cabassous centralis*).

Perhaps most striking result was the frequency at which we photographed domestic dogs. Even after excluding dogs that were associated with humans, domestic dogs were the second most frequently photographed animal in our study area (Figure 8). More interesting still, many of the coyotes that we photographed possessed distinctly dog-like traits such as shortened tails, hound-like facial profiles, and variable, dog-like pelage (Figure 9). Similar traits have also been reported in northeastern Costa Rica, another area recently colonized by coyotes (Cove et al. 2012). It appears likely that coyotes in eastern Panama are hybridizing with free roaming dogs, although further genetic testing will be needed to confirm this.

DISCUSSION

Rapid habitat conversion in Central America may be opening up new wave of biotic interchange, allowing species that are adapted to non-forest habitats to move between North and South America. The coyote and crab-eating fox may be the first mammals to exploit this expanding corridor of human disturbance. The ecological implications of this expansion are unclear, but could be serious, even in degraded habitats. Mammal communities in Panama's agricultural lands are already disturbed by habitat fragmentation, but several rare species persist on the landscape, including giant anteaters, greater grisons, and naked-tailed armadillos. The addition of two new mesopredators into the ecosystem in addition to an existing population of free-roaming dogs could place additional pressures on already struggling populations. In particular, small native predators and small herbivores may be at risk of competition or predation.

If the species were to expand further into naturally occurring open habitats in North and South America, the conservation implications could be even greater. For coyotes, the dense forests of Darién are thought to represent a barrier between Central and South America (Hidalgo-Mihart, Cantú-Salazar, González-Romero, & López-González, 2004; Vaughan, 1983). However, parts of this barrier are now being cleared for agriculture, potentially allowing coyotes to colonize savannah ecosystems in South America. Judging from the species' success in novel North American habitats, such an event could represent a major

species invasion. Likewise, the northern expansion of the crab-eating fox could affect native carnivores and small mammal populations.

Understanding habitat preferences of coyotes and crab-eating foxes in Central America allows us to predict whether such an expansion might occur, and where the species might go. We explored this topic using data fusion models. This novel approach allowed us to pool data from several sources while acknowledging uncertainty and differences in how the information was collected. This represents a valuable improvement over existing methods. The sparseness of coyote and fox detections limited our analysis, but our models still provide some insight into their habitat preferences. Selected covariates suggest some preferential use for non-forested locations, particularly at a fine scale. Distance from previous range boundaries also emerged as an important covariate for crab-eating foxes, suggesting that they are still in the early stages of colonizing Panama.

Interactions between coyotes and crab-eating foxes are equally important. Competition between the species could potentially limit their expansion, where otherwise suitable habitat might exist. Previous studies suggest that the two species have similar dietary preferences, consuming fruits and small to medium-sized mammals (Bueno & Motta-Junior, 2004; Janzen, 1983; Juarez & Marinho, 2002; Vaughan & Rodriguez, 1986). Coyotes may take or scavenge some larger prey items than the crab-eating fox, but their dietary habits are generally similar. In this study, we also observed high overlap in their temporal activity patterns. Both species were mostly nocturnal, with minor differences. We did, however, observe some evidence of fine-scale spatial avoidance between coyotes and crab-eating foxes

where their ranges overlap. If coyotes or crab-eating foxes continue to expand, we might predict spatial avoidance to play an important role in reducing competition between the two species where they co-occur.

Characterizing range expansions such as these during their early stages is important for conservation. However, as our study exemplifies, statistically analyzing such expansions can be logistically challenging. Low detectability may be expected due to low population density, reducing the number of detections and increasing required survey effort. Furthermore, occupancy signals can be weak in early stages of colonization and range expansion, making habitat preferences difficult to determine (Yackulic et al., 2015). Novel approaches such as data fusion, particularly when used in conjunction with replicate surveys through time, could provide a valuable tool for offsetting some of these challenges.

REFERENCES

- Bueno, A. D. A., & Motta-Junior, J. C. (2004). Food habits of two syntopic canids, the maned wolf (*Chrysocyon brachyurus*) and the crab-eating fox (*Cerdocyon thous*), in southeastern Brazil. *Revista Chilena de Historia Natural*, 77(1), 5–14.
<http://doi.org/10.4067/S0716-078X2004000100002>
- Cuervo Díaz, A., Hernández-Camacho, J. I., & Cadena, A. (1986). Lista actualizada de los mamíferos de Colombia: Anotaciones sobre su distribución. *Caldasia*, 15, 471–501.
- Di Bitetti, M. S., Di Blanco, Y. E., Pereira, J. a., Paviolo, A., & Pérez, I. J. (2009). Time partitioning favors the coexistence of sympatric crab-eating foxes (*Cerdocyon thous*) and pampas foxes (*Lycalopex gymnocercus*). *Journal of Mammalogy*, 90(2), 479–490.
<http://doi.org/10.1644/08-MAMM-A-113.1>
- Efford, M. G., & Dawson, D. K. (2012). Occupancy in continuous habitat. *Ecosphere*, 3(4), 32. <http://doi.org/10.1890/ES11-00308.1>
- FAO. (2015). *Global Forest Resources Assessment 2015*. Rome, Italy.
- Gerber, B. D., Karpanty, S. M., & Kelly, M. J. (2012). Evaluating the potential biases in carnivore capture-recapture studies associated with the use of lure and varying density estimation techniques using photographic-sampling data of the Malagasy civet. *Population Ecology*, 54(1), 43–54. <http://doi.org/10.1007/s10144-011-0276-3>
- Hadik-Barkoczy, L. B. (2013). First camera trap record of crab-eating fox on Auyan Tepui, Venezuela. *Canid Biology and Conservation*, 16(4), 12–15.
- Hansen, M. C., Potapov, P. V, Moore, R., Hancher, M., Turubanova, S. A., Tyukavina, A.,

- ... Townshend, J. R. G. (2013). High-resolution global maps of 21st-century forest cover change. *Science*, *342*(2013), 850–853. <http://doi.org/10.1126/science.1244693>
- Hidalgo-Mihart, M. G., Cantú-Salazar, L., González-Romero, A., & López-González, C. A. (2004). Historical and present distribution of coyote (*Canis latrans*) in Mexico and Central America. *Journal of Biogeography*, *31*(12), 2025–2038. Retrieved from <http://dx.doi.org/10.1111/j.1365-2699.2004.01163.x>
- Hijmans, R. J., Cameron, S. E., Parra, J. L., Jones, P. G., & Jarvis, A. (2005). Very high resolution interpolated climate surfaces for global land areas. *International Journal of Climatology*, *25*(15), 1965–1978. <http://doi.org/10.1002/joc.1276>
- Hofmeester, T. R., Rowcliffe, J. M., & Jansen, P. A. (2016). A simple method for estimating the effective detection distance of camera traps. *Remote Sensing in Ecology and Conservation*. <http://doi.org/10.1002/rse2.25>
- Janzen, D. H. (1983). *Canis latrans* (coyote). In *Costa Rican natural history* (pp. 456–457). Chicago, IL, USA: University of Chicago Press.
- Juarez, K. M., & Marinho, J. (2002). Diet, habitat use, and home ranges of sympatric canids in central Brazil. *Journal of Mammalogy*, *83*(4), 925–933. [http://doi.org/10.1644/1545-1542\(2002\)083<0925:Dhuahr>2.0.Co;2](http://doi.org/10.1644/1545-1542(2002)083<0925:Dhuahr>2.0.Co;2)
- Kays, R., Curtis, A., & Kirchman, J. J. (2010). Rapid adaptive evolution of northeastern coyotes via hybridization with wolves. *Biology Letters*, *6*(1), 89–93. <http://doi.org/10.1098/rsbl.2009.0575>
- Leigh, E. G., O’Dea, A., & Vermeij, G. J. (2014). Historical biogeography of the Isthmus of

- Panama. *Biological Reviews*, 89(1), 148–172. <http://doi.org/10.1111/brv.12048>
- Lunn, D. J., Thomas, A., Best, N., & Spiegelhalter, D. (2000). WinBUGS – A Bayesian modelling framework: Concepts, structure, and extensibility. *Statistics and Computing*, 10, 325–337. <http://doi.org/10.1023/A:1008929526011>
- Macdonald, D. W., & Courtenay, O. (1996). Enduring social relationships in a population of crab-eating zorros, *Cerdocyon thous*, in Amazonian Brazil (Carnivora, Canidae). *Journal of Zoology, London*, 239(2), 329–355.
- Macdonald, D. W., & Sillero-Zubiri, C. (2004). *The biology and conservation of wild canids*. New York, NY, USA: Oxford University Press Inc., New York.
- MacFadden, B. J. (2006). Extinct mammalian biodiversity of the ancient New World tropics. *Trends in Ecology and Evolution*, 21(3), 157–165.
<http://doi.org/10.1016/j.tree.2005.12.003>
- MacKenzie, D. I., Nichols, J. D., Lachman, G. B., Droege, S., Royle, J. A., & Langtimm, C. A. (2002). Estimating site occupancy rates when detection probabilities are less than one. *Ecology*, 83(8), 2248–2255.
- MacKenzie, D. I., Nichols, J. D., Royle, J. A., Pollock, K. H., Bailey, L. L., & Hines, J. E. (2006). *Occupancy estimation and modeling: Inferring patterns and dynamics of species occurrence* (1st ed.). Burlington, MA, USA: Elsevier Academic Press.
- Marshall, L. G., Webb, S. D., Sepkoski, J. J., & Raup, D. M. (1982). Mammalian evolution and the Great American Interchange. *Science*, 215(4538), 1351–1357.
- Méndez, E., Delgado, F., & Miranda, D. (1981). The Coyote (*Canis latrans*) in Panama.

International Journal for the Study of Animal Problems, 2(5), 252–255.

Méndez-Carvajal, P., & Moreno, R. (2014). Mammalia, Carnivora, Canidae, *Canis latrans* (Say, 1893): Actual distribution in Panama. *Check List*, 10(2), 376–379.

Meyer, N. F. V., Esser, H. J., Moreno, R., van Langevelde, F., Liefjing, Y., Oller, D. R., ... Jansen, P. A. (2015). An assessment of the terrestrial mammal communities in forests of Central Panama, using camera-trap surveys. *Journal for Nature Conservation*, 26, 28–35. <http://doi.org/10.1016/j.jnc.2015.04.003>

Moore, G. C., & Parker, G. R. (1992). Colonization by the eastern coyote (*Canis latrans*). In A. H. Boer (Ed.), *Ecology and management of the eastern coyote* (pp. 23–38). Fredericton, New Brunswick, Canada: Wildlife Research Unit, University of New Brunswick.

NatureServe, & IUCN (International Union for Conservation of Nature). (2015). *Cerdocyon thous*. In: *The IUCN Red List of Threatened Species* (Version 2015.3). Retrieved June 29, 2015, from <http://iucnredlist.org>

NatureServe, & IUCN (International Union for Conservation of Nature). (2016). *Cerdocyon thous*. In: *The IUCN Red List of Threatened Species* (Version 2016.4). Retrieved February 02, 2016, from <http://iucnredlist.org>

Olsoy, P. J., Zeller, K. A., Hicke, J. A., Quigley, H. B., Rabinowitz, A. R., & Thornton, D. H. (2016). Quantifying the effects of deforestation and fragmentation on a range-wide conservation plan for jaguars. *Biological Conservation*, 203(January), 8–16. <http://doi.org/10.1016/j.biocon.2016.08.037>

- Pacifici, K., Reich, B., Miller, D., Gardner, B., Glenn, S., Singh, S., ... Collazo, J. (2016). Integrating multiple data sources in species distribution modeling: a framework for data fusion. *Ecology*. <http://doi.org/10.13140/RG.2.1.3702.8566>
- Parker, G. (1995). Colonization. In *Eastern coyote: the story of its success* (pp. 16–35). Halifax, Nova Scotia: Nimbus Publishing.
- Ramírez-Chaves, H. E., & Pérez, W. A. (2015). New record of crab-eating fox in southwestern Colombia , with comments on its distribution in Colombia and Ecuador. *Canid Biology & Conservation*, 18(3), 6–9.
- Reid, F. A. (2006). *A field guide to mammals of North America north of Mexico* (4th ed.). New York, NY, USA: Houghton Mifflin Company.
- Rowcliffe, J. M. (2016). activity: Animal activity statistics (Version 1.1) [computer software]. Available at <https://cran.r-project.org/package=activity>
- Schank, C., Mendoza, E., García Vettorazzi, M. J., Cove, M. V., Jordan, C. A., O’Farrill, G., ... Leonardo, R. (2015). Integrating current range-wide occurrence data with species distribution models to map the potential distribution of Baird’s tapir. *Tapir Conservation*, 24(33), 15–25. <http://doi.org/10.5281/zenodo.23417>
- Simpson, G. G. (1980). *Splendid isolation: the curious history of South American mammals*. New Haven, CT, USA: Yale University Press.
- Spiegelhalter, D. J., Best, N. G., Carlin, B. P., & van der Linde, A. (2002). Bayesian measures of model complexity and fit. *Journal of the Royal Statistical Society Series B (Statistical Methodology)*, 64(4), 583–639. <http://doi.org/10.1111/1467-9868.00353>

- Springer, M. T., Carver, A. D., Nielsen, C. K., Correa, N. J., Ashmore, J. R., Ashmore, J. R., & Lee, J. G. (2012). Relative Abundance of Mammalian Species in a Central Panamanian Rainforest. *Revista Latinoamericana de Conservación*, 2(2), 19–26.
- Tchaicka, L., Eizirik, E., De Oliveira, T. G., Cândido, J. F., & Freitas, T. R. O. (2007). Phylogeography and population history of the crab-eating fox (*Cerdocyon thous*). *Molecular Ecology*, 16(4), 819–838. <http://doi.org/10.1111/j.1365-294X.2006.03185.x>
- Tejera, V. H., Araúz, J., León, V., Rodríguez, A. R., González, P., Bermúdez, S., & Moreno, R. (1999). Primer registro del zorro cangrejero, *Cerdocyon thous* (Carnivora: Canidae), Para Panamá. *Scientia*, 14(2), 103–107.
- Thoisy, B. De, Vergara, M., Silvestro, P., & Vasconcelos, I. (2013). Distribution Update Northern extension of records of the crab-eating fox in Brazil. *Canid Biology & Conservation*, 16(1), 1–3.
- Vaughan, C. (1983). Coyote range expansion in Costa Rica and Panama. *Brenesia*, 21, 27–32.
- Vaughan, C., & Rodriguez, M. (1986). Comparación de los hábitos alimentarios del coyote (*Canis latrans*) en dos localidades en Costa Rica. *Vida Silvestre Neotropical*, 1(1), 6–11.
- Wallace, A. R. (1876). The geographical distribution of animals: With a study of the relations of living and extinct faunas as elucidating the past changes of the earth's surface. New York, NY, USA: Harpers.
- Yackulic, C. B., Nichols, J. D., Reid, J., & Der, R. (2015). To predict the niche, model colonization and extinction. *Ecology*, 96(1), 16–23. <http://doi.org/10.1890/14-1361.1>

Table 1. DIC results for top five crab-eating fox (*Cerdocyon thous*) data fusion models. Model covariates are defined as follows: ‘distance’=distance past c.2000 range boundary, ‘bait’=whether individual camera traps were baited/non-baited, ‘forest’=whether individual camera traps were deployed in forest/non-forest locations, ‘tree cover’=cell percent forest cover, ‘bc07’=cell annual temperature range (BIOCLIM-7), ‘bc16’=cell wet season precipitation (BIOCLIM-16), ‘+’ denotes an additive effect, and ‘.’ denotes no covariates. The top four models have competing support under DIC, but significantly outperform all other models. The top three models are nearly indistinguishable ($\Delta\text{DIC} < 5$), and the fourth model is competitive ($\Delta\text{DIC} < 10$) but less well-supported than the top three. The fitted models suggest that occupancy and GBIF records of crab-eating foxes become less common with westward distance into Panama. GBIF records may also occur less frequently in wetter, forested sites with pronounced seasonality, although the support for this is uncertain due to similarities in model DIC. In occupied sites, baited cameras deployed in non-forest locations detected crab-eating foxes more readily than non-baited cameras or cameras deployed in forested locations.

<i>Occupancy</i> (ψ)	Model Covariates		DIC	pD	ΔDIC
	<i>Detectability</i> (p)	<i>GBIF Probability</i> (p_{GBIF})			
.	bait + forest	distance + tree cover	185.01	23.96	0.00
.	bait + forest	distance + bc07 + bc16	185.24	25.20	0.23
.	bait + forest	distance	185.71	24.36	0.70
distance	bait + forest	distance + tree cover	191.04	26.48	6.03
.	bait + forest	tree cover	198.53	24.11	13.52

Table 2. DIC results for top five coyote (*Canis latrans*) occupancy models. Covariates are defined as follows: ‘roadkill’= smoothed roadkill frequency (25-km radius) within cell, ‘tree cover’ = percent tree cover within cell, ‘bait’ = whether individual camera traps were baited/non-baited, ‘forest’ = whether individual camera traps were deployed in forest/non-forest habitat, ‘survey’ = whether individual camera traps were deployed in the 2015 survey or a recent collaborator survey. The top two models received indistinguishable support ($\Delta\text{DIC} < 5$), and the third model was competitive ($\Delta\text{DIC} < 10$) but less well-supported.

Model Covariates		DIC	pD	ΔDIC
<i>Occupancy</i> (ψ)	<i>Detectability</i> (p)			
roadkill	bait + forest	108.99	18.83	0.00
roadkill + tree cover	bait + forest	109.42	17.08	0.43
.	bait + forest + survey	116.70	25.32	7.71
.	bait + forest	119.93	29.22	10.94
.	bait + survey	121.58	27.62	12.59

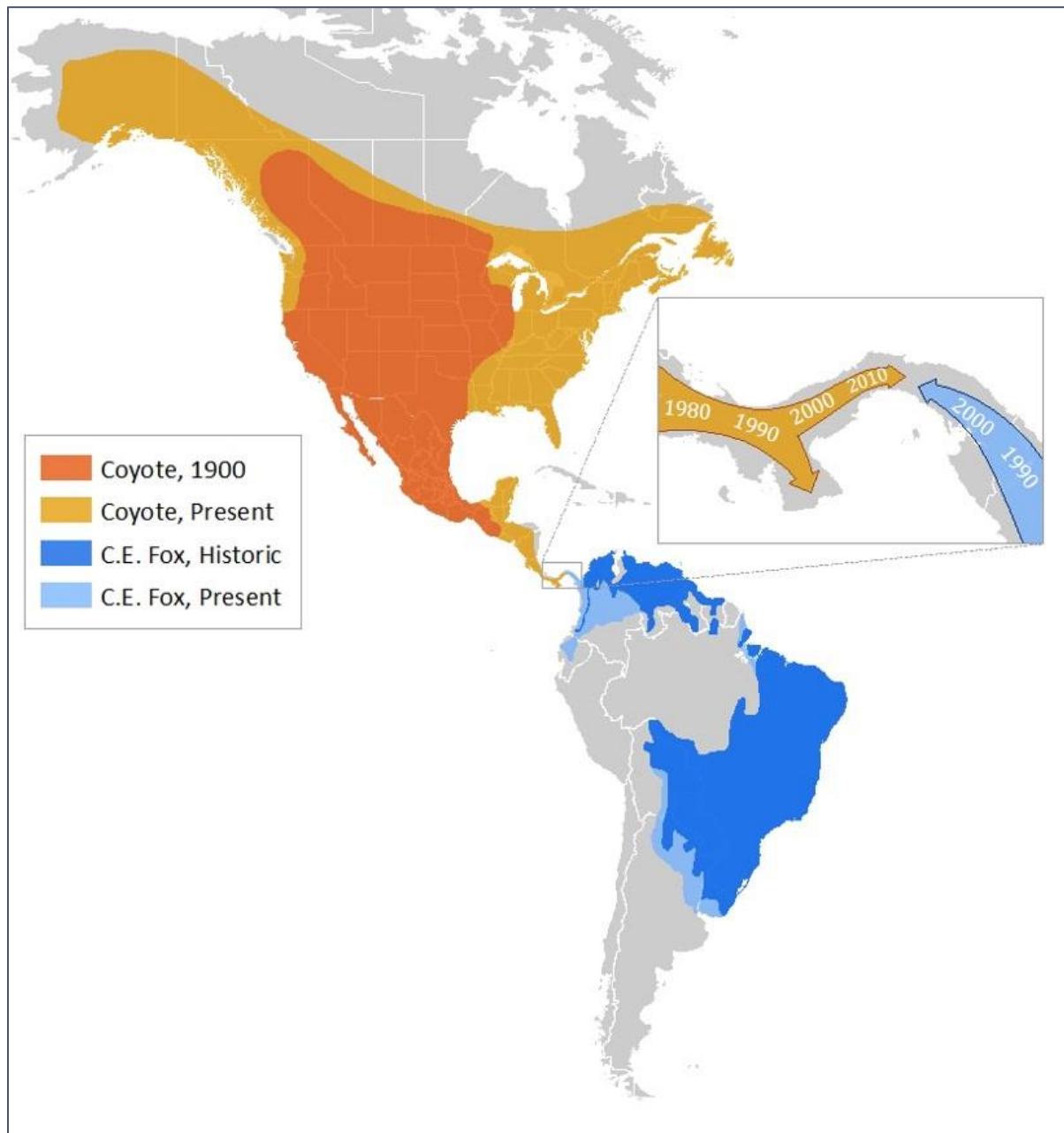


Figure 1. Contemporary range expansion by coyotes (*Canis latrans*) and crab-eating foxes (*Cerdocyon thous*) in response to human disturbances. Both species have recently colonized agriculture-dominated landscapes in Panama, bringing them into contact for the first time. Continent-wide coyote range expansion based on historical records collected between 1850 and 2016 (Hody & Kays, *in prep*), and continent-wide crab-eating fox range expansion based on IUCN range estimates (NatureServe & IUCN, 2015, 2016). Range expansions in Panama based on the published literature (Reid 2006; Méndez-Carvajal & Moreno 2014).

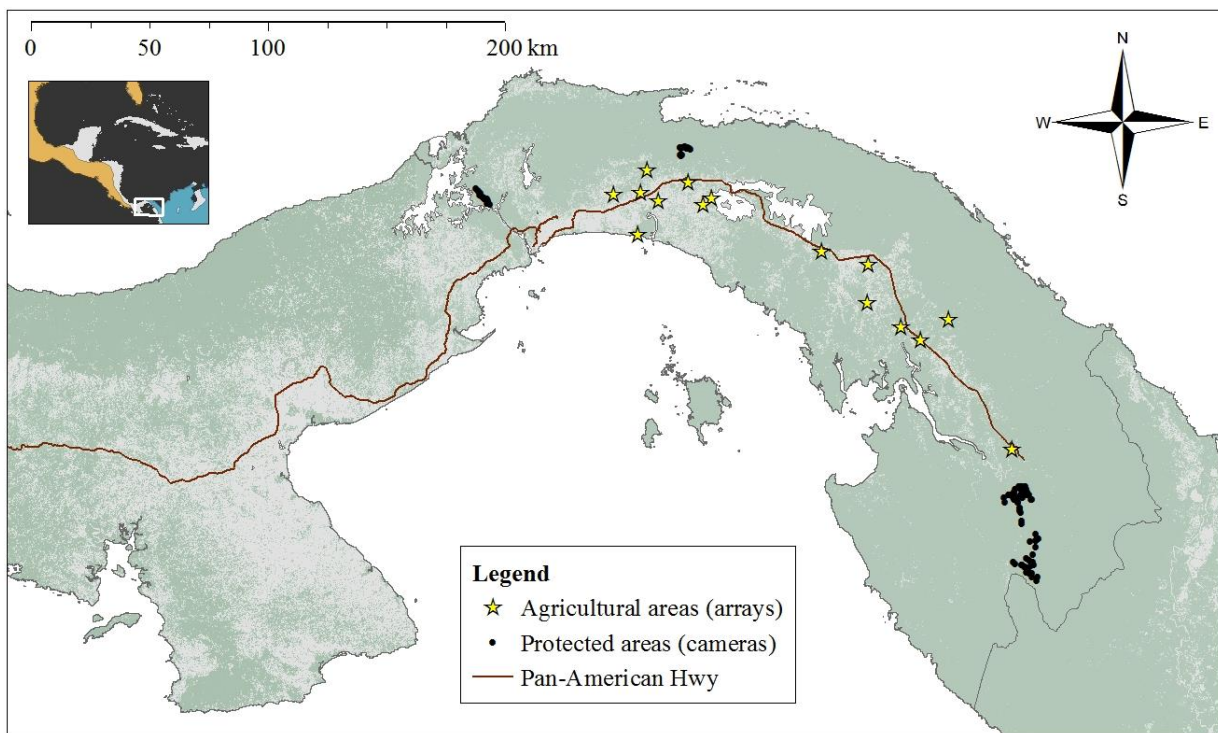


Figure 2. Camera trap deployments in eastern Panama. Green area denotes forest cover as of 2000. Camera traps were placed in small arrays in an agricultural corridor along the Pan-American Highway during March – June 2015 through collaborations with local landowners. Camera traps were also placed in four adjacent protected areas during 2005 – 2015 by our collaborators Ricardo Moreno and Ninon Meyer.

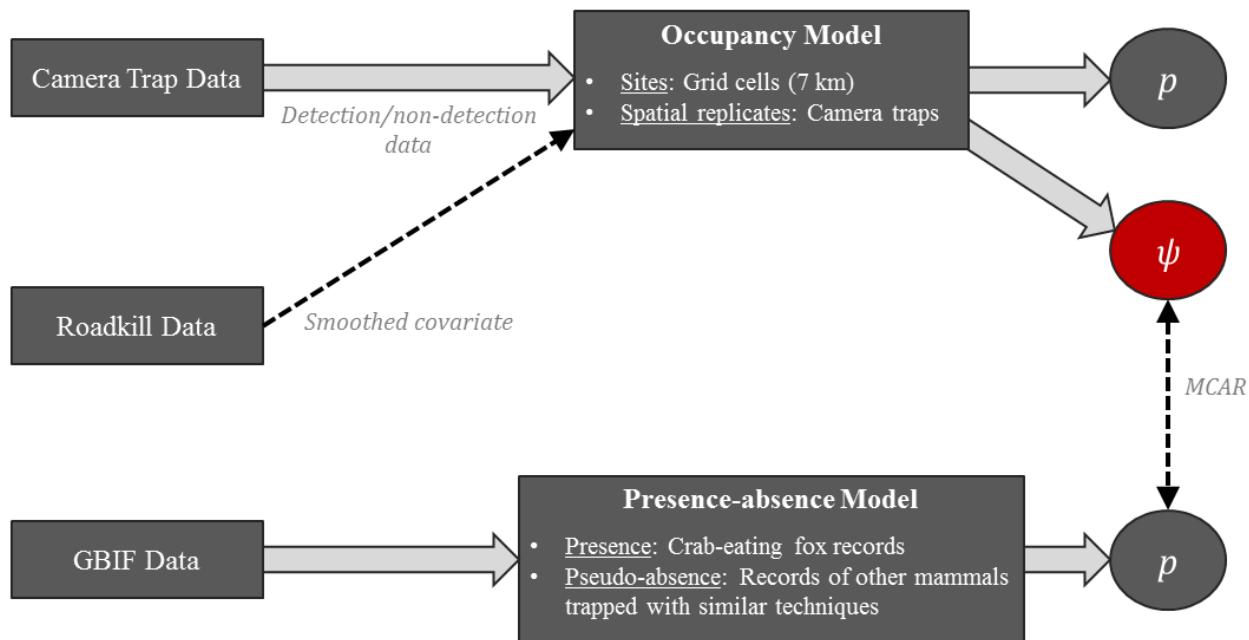


Figure 3. Diagram of data fusion model. Camera trap, roadkill, and GBIF data are analyzed together to estimate occupancy probability on a 7-km hexagonal grid. The data fusion model consists of two sub-models. Camera trap data acts as the primary data source, analyzed in an occupancy sub-model that treats grid cells as sites, and individual camera traps as spatial replicates within the cells. Roadkill data is integrated into this sub-model as a spatially-smoothed covariate. GBIF data acts as a secondary data source, analyzed in a presence-absence sub-model that also treats cells as sites. Here, crab-eating fox records act as presence data, and records of similar-sized non-arboreal terrestrial mammals are treated as pseudo-absences. Probability of occupancy (ψ) and probability of observing a crab-eating fox record in GBIF (p_{GBIF}) both include spatial random effects terms, defined using a multivariate CAR (MCAR) distribution that links the two sub-models.

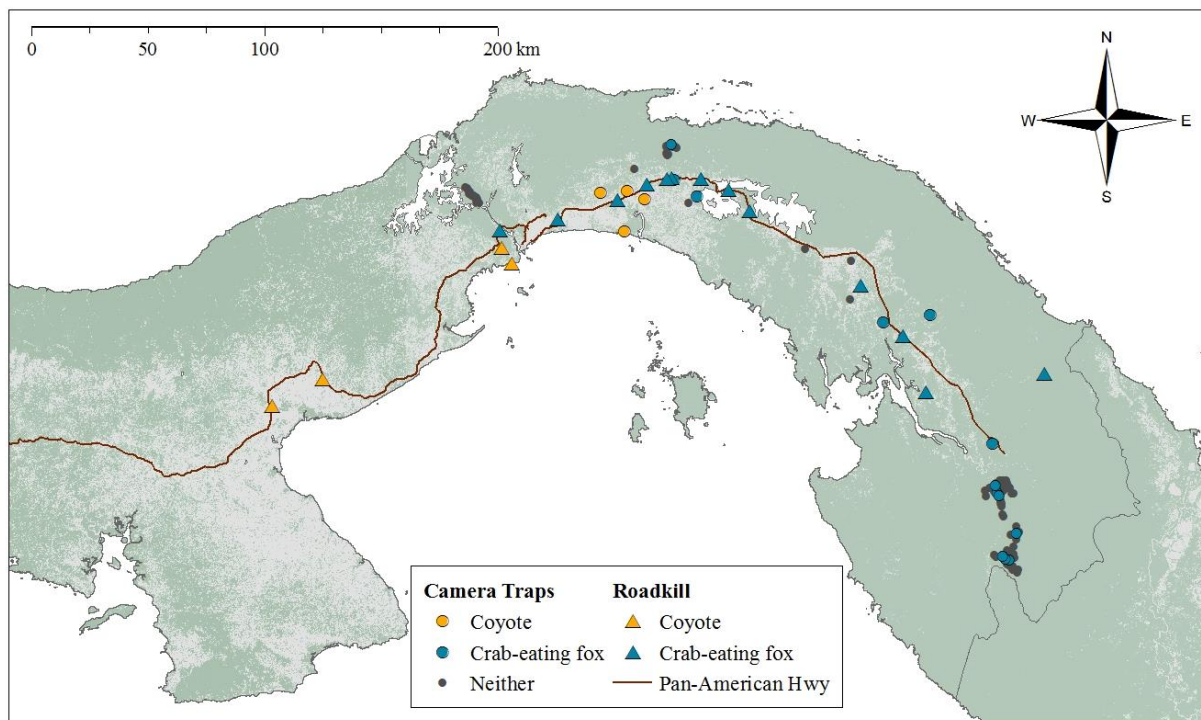


Figure 4. Locations of camera deployments and detections of coyote and crab-eating foxes. Green area denotes forest cover as of 2000. Camera deployments spanned a 250-km long agricultural corridor along the Pan-American Highway and four protected forests across eastern Panama. Coyotes were only detected in the western portion of the study area, extending about 70 km west of the Panama Canal. Crab-eating foxes were detected in forested and agricultural habitats across eastern Panama.

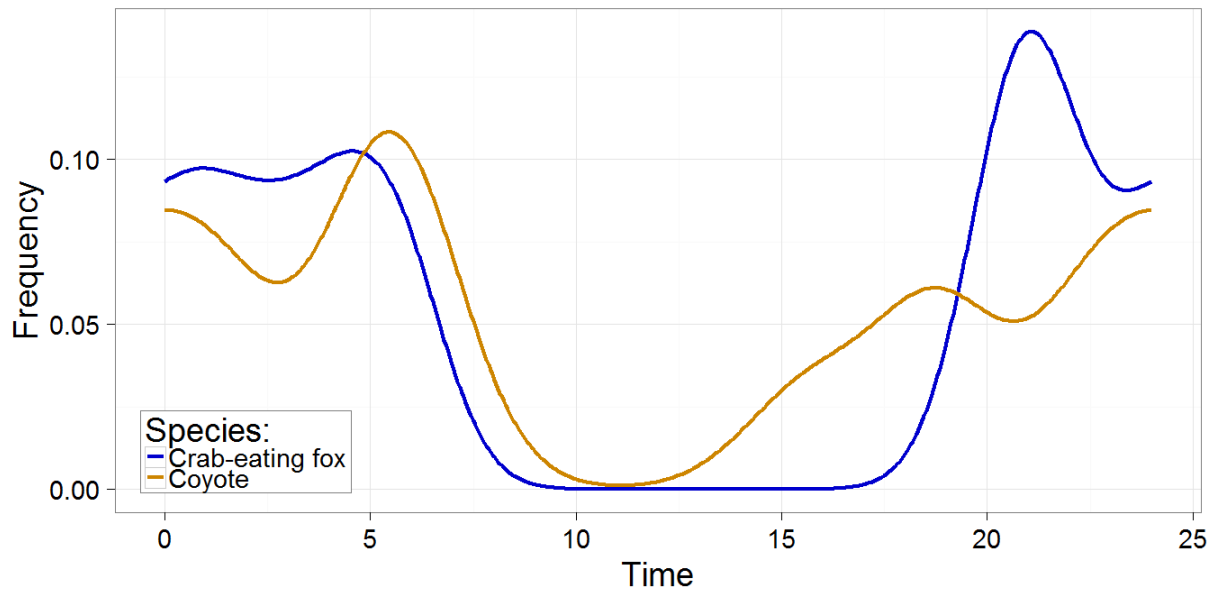


Figure 5. Daily distribution of coyote and crab-eating fox photographs during camera trap survey in spring 2015. Curves were fitted using circular kernel density estimators in the R-package ‘activity’ (Rowcliffe, 2016). Both species are nocturnal in eastern Panama, although coyotes appear to be active earlier in the evening and later in the morning than the foxes. General activity patterns of the crab-eating fox closely resemble those reported in South America, including the peak in activity just after dusk (Di Bitetti, Di Blanco, Pereira, Paviolo, & Pérez, 2009; D. W. Macdonald & Courtenay, 1996).

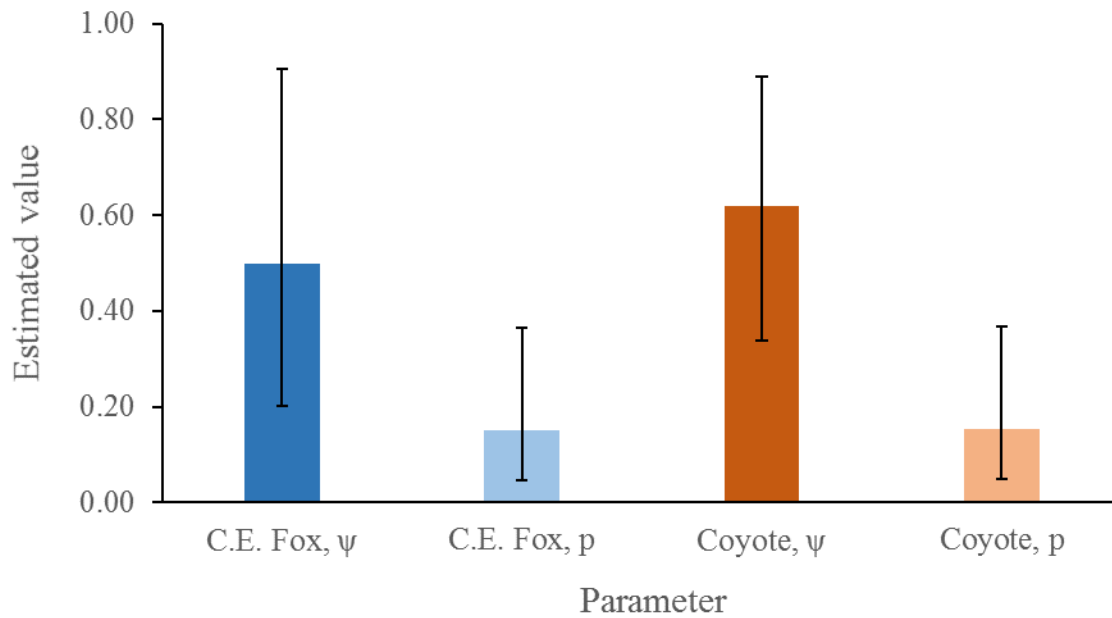


Figure 6. Parameter estimates for coyotes and crab-eating foxes in eastern Panama. Bars represent medians and 95% credible intervals based on the posterior distributions of the intercept values for occupancy and detection probability in the highest-ranked model for each species. Detection probability (p) is the probability of detecting a coyote or fox at an individual camera during a 21-day deployment, and occupancy probability (ψ) is the probability of a coyote or fox occupying a 7-km grid cell.

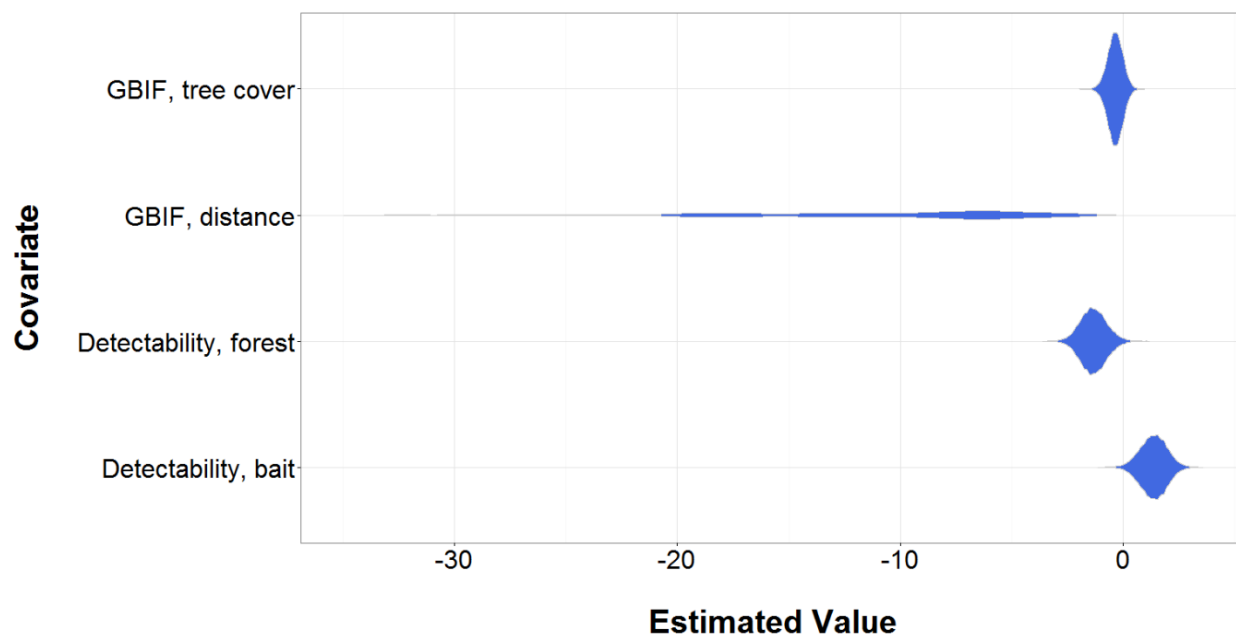


Figure 7. Posterior distributions of covariate effects for top crab-eating fox model. Tree cover and distance from the c.2000 range boundary had negative effects on the probability of observing a GBIF record of a crab-eating fox (p_{GBIF}), although the effect of distance was modeled with high uncertainty. In the occupancy sub-model, forest cover had a negative effect on detection probability (p), and bait status had a positive effect on detection probability.

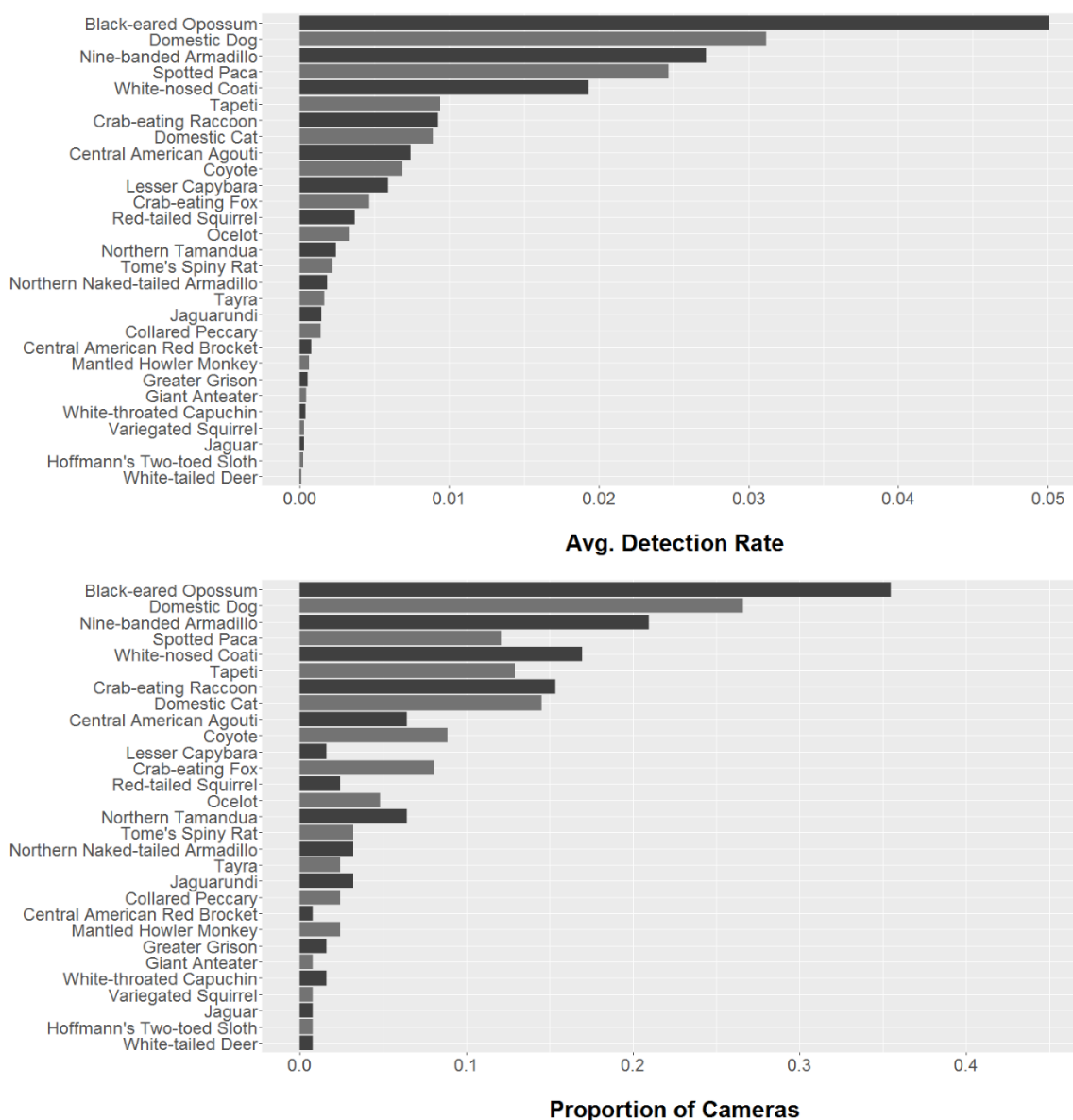


Figure 8. Summary of mammal communities in disturbed habitats in eastern Panama. ‘Average detection rate’ is defined as the number of photo sequences per day, averaged across all camera traps. ‘Proportion of cameras’ denotes the proportion of all cameras that photographed the species at least once. Additional notes: (1) Domestic animals and humans are omitted from the figure, with the exception of domestic dogs and domestic cats. (2) Dog detections were only included if they occurred ≥ 5 minutes before or after detection of a human in order to better estimate the occurrence of free roaming dogs. Domestic cattle, horses, and sheep were not counted.



Figure 9. Coyotes from in eastern Panama. Many of the coyotes that were photographed in eastern Panama had distinctly dog-like traits, including hound-like facial profiles, shortened tails, and variable dog-like pelage. These traits suggest that local coyote populations may be hybridizing with free roaming dogs.

APPENDICES

Appendix A

Fine-scale temporal correlograms for animal detections in Schenck Forest

Prior to analysis, we used the JMP Pro 12 Time Series Analysis platform (SAS, 2015) to study temporal autocorrelation and partial autocorrelation in animal detections. We analyzed the detections two ways. First, we considered autocorrelation between any animal detections, regardless of species. Second, we considered autocorrelation between detections within individual species with at least $n=30$ photo sequences. In both cases, we collapsed data into minute-by-minute detection histories, where '1' denotes detection anywhere on the grid and '0' denotes no detections on the grid for a given minute. We considered different time lags for the two scenarios. When fitting the multispecies correlograms, we considered a maximum time lag of 60 min and a forecasting period of 25 min. When fitting the single-species correlograms, we reduced the maximum time lag to 30 min. All other settings remained the same. We judged temporal autocorrelation to be insignificant when it consistently dropped within ± 2 standard deviations of 0.

Temporal autocorrelation of all species combined persisted up to 40 minutes, but autocorrelation for individual species dissipated more quickly. Autocorrelation dissipated within 5 minutes for gray squirrels, raccoons, and coyotes, and dissipated within 20 minutes and 26 minutes for opossums and white-tailed deer. We selected to use a 5 minute grouping rule since it is more conservative and reduces the chances of grouping unrelated photographs.

Table 1. Results of time series analyses on animal detections.

Species	Max. Time Lag (min)	Forecasting (min)	Threshold (min)
All (combined)	60	25	40
White-tailed deer	30	25	26
Eastern gray squirrel	30	25	3
Virginia opossum	30	25	20
Northern raccoon	30	25	5
Coyote	30	25	5

Appendix B

Assignment of missed detections in Schenck Forest and general trends in trigger probability

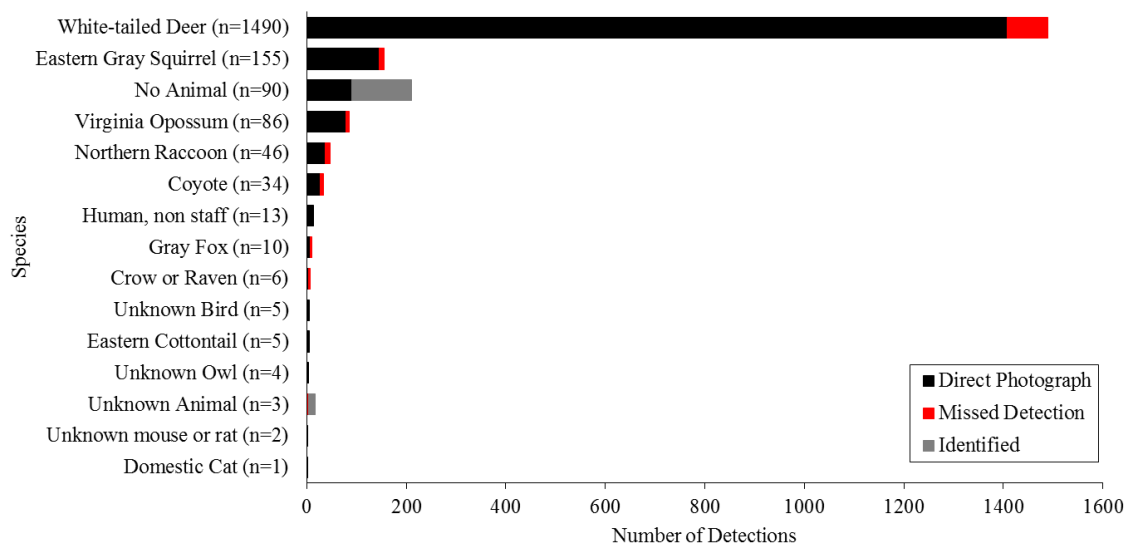


Figure 1. Summary of photographs, including putative missed detections. “Direct photograph” describes the number of unique images in which the species occurs within the frame. “Missed detection” describes the number of unique images where the animal triggered the camera, but moved out of the frame, making the image empty or unidentifiable. “Identified” describes the number of ‘no animal’ and ‘unidentifiable animal’ photographs that could be attributed to an animal species based on the 5-minute heuristic rule. Sample sizes (direct photographs and missed detections combined) are included alongside the species names.

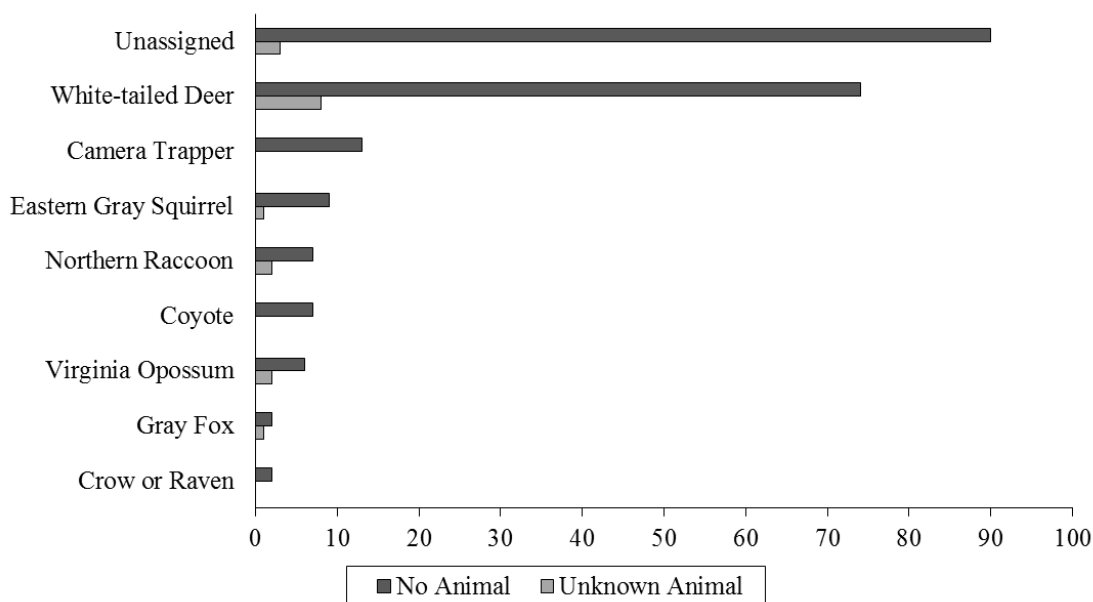


Figure 2. Assignment of "no animal" and "unknown animal" photographs. One "no animal" photograph was associated with a movement path of "unknown animal" photographs and was therefore reclassified as an "unknown animal" photograph.

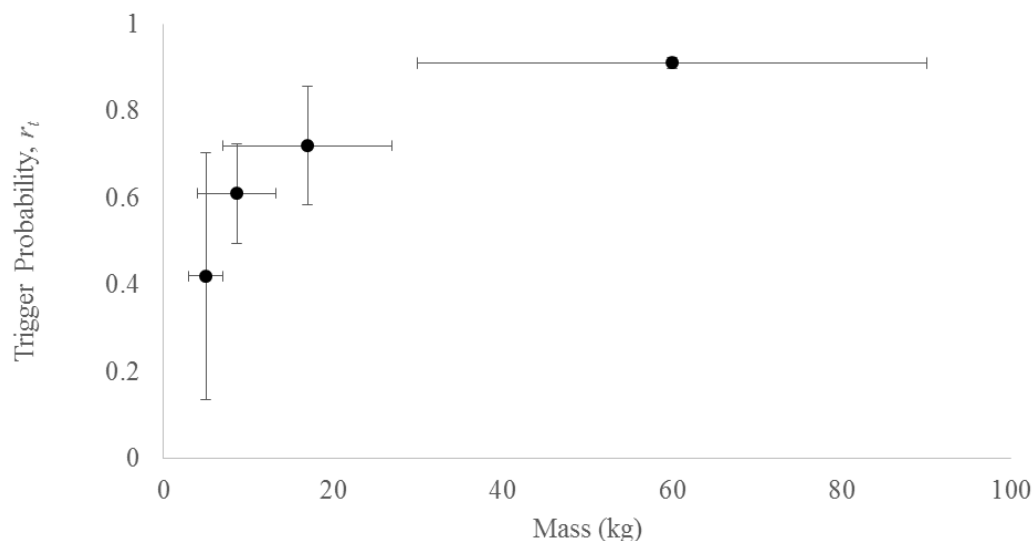


Figure 3. Trigger probability vs. body mass. Body masses based on those presented in Mammals of North America (Kays & Wilson, 2009). We observe a general increase in estimated trigger probability as the body mass of the species increases.

Appendix C

Annotated BUGS code for broad-scale occupancy models

```

model{
#####
# LIKELIHOOD:
for(i in 1:N) {

  # STATE MODEL:
  z[i] ~ dbern(psi[i]) # Occupancy state.
  logit(psi[i]) <- b0 # Occupancy probability.

  # DETECTION MODEL:
  Y[i] ~ dbin(muy[i],J[i]) # Detection given occupancy.
  logit(p[i]) <- a0 + a1*trail[i] + err[i]
  muy[i] <- z[i]*p[i]
}

#####
# PRIORS FOR DETECTABILITY:

a0 ~ dnorm(0.0, 0.01) # Baseline detectability
a1 ~ dnorm(0.0, 0.01) # Detectability, effect of trail

for(i in 1:N) {
  err[i] ~ dnorm(0.0, err.tau) # Random effects term
}
err.tau ~ dgamma(1,1) # Hyperparameter: Inv. variance of RE
err.sd <- sqrt(1/err.tau) # Get st.dev. from inv. variance

# PRIORS FOR OCCUPANCY:
b0 ~ dnorm(0.0, 0.001) # Baseline occupancy

#####
# PROBABILITY OF DRAWING THE EMPIRICALLY-DERIVED P
alpha.test ~ dnorm(a0, err.tau) # Draw based on a0, err.tau
logit(p.test) <- alpha.test
}

```

Appendix D

Sampling effort for camera arrays and grid cells in eastern Panama

Table 1. Description of camera trap arrays in eastern Panama. “Site type” specifies whether a camera array was deployed within the agricultural corridor surrounding the Pan-American Highway (‘agricultural’) or an adjacent protected area (‘protected’). “Lat.” and “long.” gives the mean latitude and longitude of the array in decimal degrees (WGS84). “No. Cameras” gives the number of camera traps that were functioning at the end of the camera deployment and thus available for analysis, and “deployment” gives the average length of time that an individual camera was left in the field, in days.

Site Name	Site Type	Year	Lat.	Long.	No. Cameras	Deployment (days)
Altas de Veronicas	Agricultural	2015	9.16	-79.25	7	34
Aguas Mansas	Agricultural	2015	9.15	-78.88	8	31
Saino	Agricultural	2015	9.01	-79.16	9	78
Maria Isabella	Agricultural	2015	9.14	-79.08	10	27
Santa Librada	Agricultural	2015	8.76	-78.29	9	30
Los Rios	Agricultural	2015	8.20	-77.74	8	21
Palmas Beya	Agricultural	2015	8.90	-78.28	10	19
Centro Pastoral	Agricultural	2015	8.67	-78.16	5	26
Altas de Cristo	Agricultural	2015	8.62	-78.09	2	26
Rio Chucunaque	Agricultural	2015	8.70	-77.98	10	27
Finca Palmera	Agricultural	2015	8.95	-78.46	10	21
La Corriente	Agricultural	2015	9.21	-78.97	3	45
Chepo	Agricultural	2015	9.25	-79.12	7	20
Las Planes	Agricultural	2015	9.13	-78.91	1	22
Gonzolillo	Agricultural	2015	9.18	-79.15	7	17
Cana - Darién	Protected	2006	7.78	-77.67	22	57
Pirre - Darién	Protected	2015	8.02	-77.71	44	71
Nusagandi	Protected	2013	9.34	-78.98	15	62
Soberanía	Protected	2013	9.15	-79.74	17	106

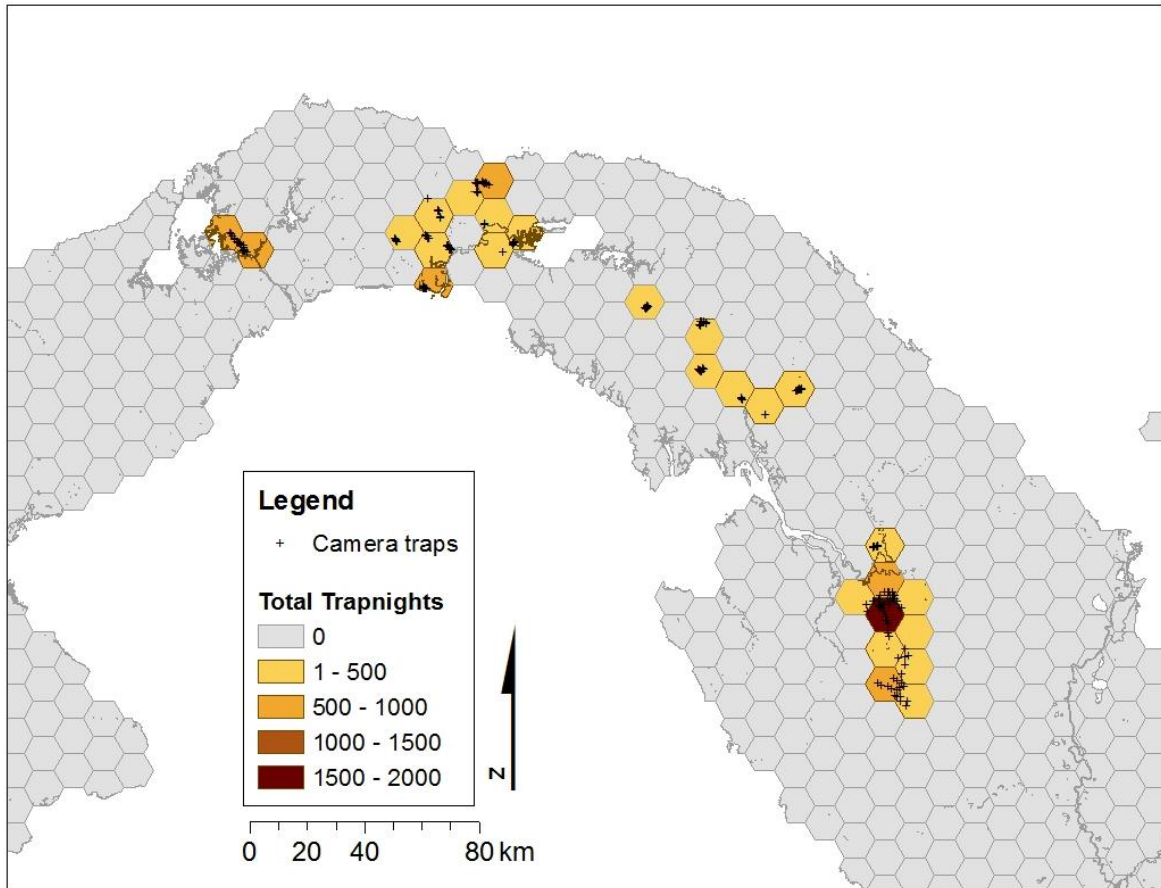


Figure 1. Camera trap survey intensity in eastern Panama by grid cell. A lattice of 7-km hexagonal grid cells was superimposed across eastern Panama to facilitate data fusion models for crab-eating foxes and coyotes. Survey effort is defined here as the total number of trap-nights within individual grid cells, i.e. the number of days worth of data that were recorded within a grid cell. Total number of trap-nights increases with average deployment length and the number of cameras within a grid cell.

Appendix E

Characteristics of camera traps during March – June 2015 deployments

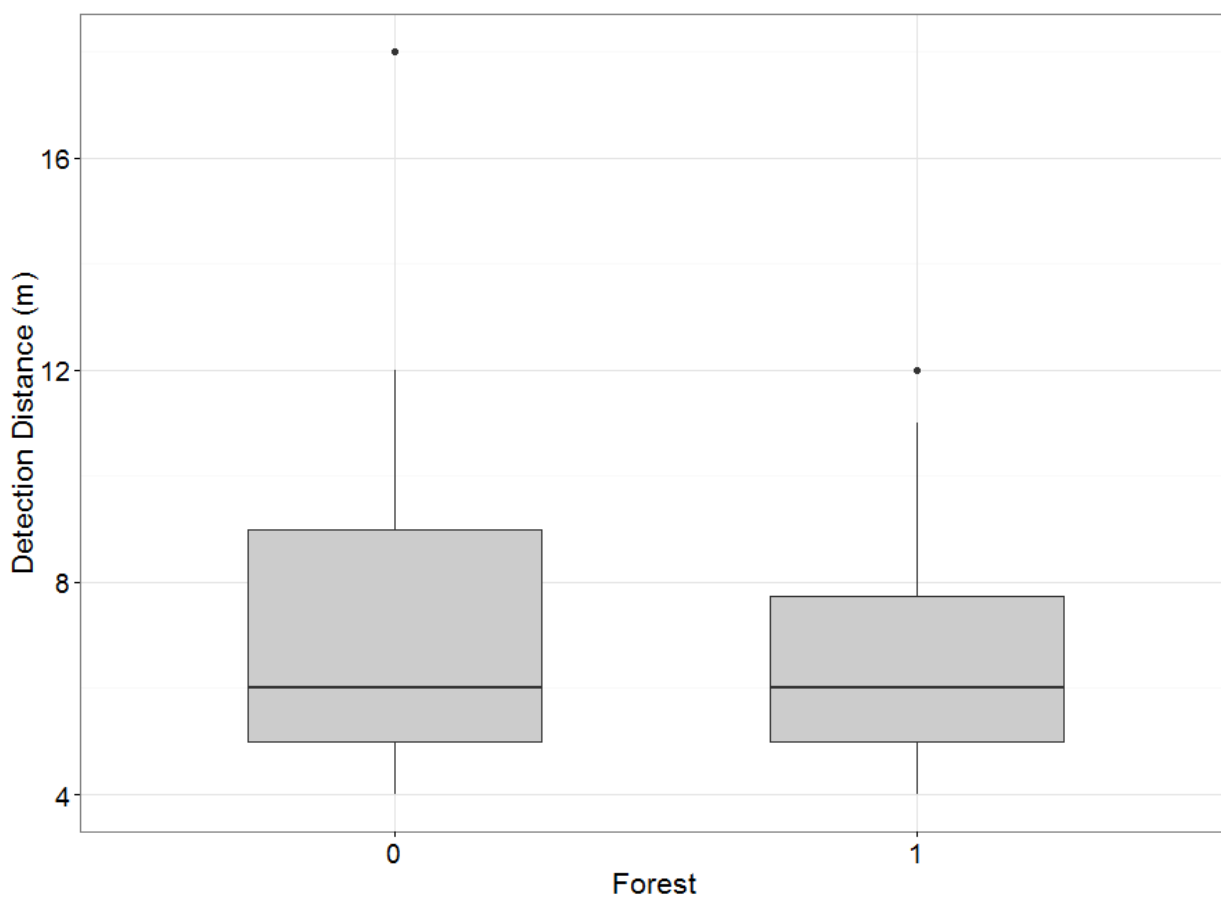


Figure 1. Box plots of observed detection distances for humans at camera traps in forested and non-forested sites. Forest=1, non-forest=0. Detection distances were estimated in the field at the time of deployment by measuring the farthest distance at which the camera PIR sensor could reliably detect a walking camera trapper. Detection distances were similar in forest and non-forest sites on average, although detection distances in non-forest sites show a positive skew in their distribution. This indicates that some non-forest camera traps could detect animals further away than forested camera traps.